Supplement of Atmos. Chem. Phys., 21, 17865–17883, 2021
https://doi.org/10.5194/acp-21-17865-2021-supplement

Atmospheric Chemistry and Physics
Open Access
EGU

Supplement of

Annual exposure to polycyclic aromatic hydrocarbons in urban environments linked to wintertime wood-burning episodes

Irini Tsiodra et al.

Correspondence to: Athanasios Nenes (athanasios.nenes@epfl.ch) and Nikolaos Mihalopoulos (nmihalo@noa.gr)

Section S1. Sampling and Analysis

Study area and sampling site

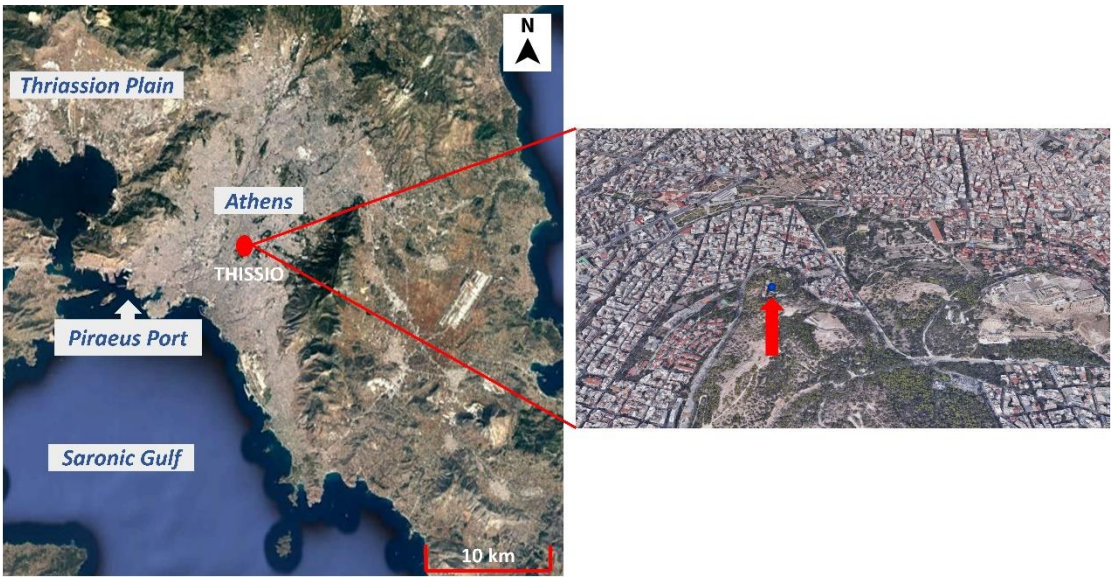

Figure S1: (Left panel) – Overview of the Greater Athens Area (GAA), with the Athens basin in the center, bordered by the Thriassion plain to the west. The red dot shows the location of the sampling site (Thissio). (Right panel) – Closer view of the site's surroundings in the historic center of Athens. Source for both images: Google Earth © , March 8 2021.

Laboratory procedures for determination of PAHs

Quartz-fiber filter samples were spiked with a mixture of deuterated internal standards ([$^2H_8$] Naphthalene, [$^2H_8$]acenaphtylene, [$^2H_{10}$]acenaphthene, [$^2H_{10}$]fluorene, [$^2H_{10}$]phenanthrene, [$^2H_{10}$]anthracene, [$^2H_{10}$]fluoranthene, [$^2H_{10}$]pyrene, [$^2H_{12}$]benzo[*a*]anthracene, [$^2H_{12}$]chrysene, [$^2H_{12}$]benzo[*b*]fluoranthene, [$^2H_{12}$]benzo[*k*]fluoranthene, [$^2H_{12}$]benzo[*a*]pyrene, [$^2H_{14}$]dibenzo[*ah*]anthracene, [$^2H_{12}$]benzo[*ghi*]perylene, [$^2H_{12}$]indeno[1,2,3-*cd*]pyrene) and solvent extracted with an accelerated solvent extraction System (Dionex ASE 300) with n-hexane - dichloromethane (50:50). The extracts were purified on a silica column, applying a modified protocol of (Parinos et al., 2019). PAHs were eluted with 10 mL n-hexane/ethyl acetate (9:1, v/v). The concentrated extract was placed into a glass vial for further concentration under a gentle nitrogen stream. [$^2H_{12}$]perylene as an internal standard, was spiked into the vial before sealing and storage.

Instrumental analysis of PAHs was carried out by an Agilent 6890N Gas Chromatographer, equipped with a 30m × 0.25mm ID × 0.25μm film thickness fused silica column (Agilent J&W DB-5MS) coupled with an Agilent Mass Selective Detector (MSD 5973, inert). The analysis was operated using a selected ion monitoring (SIM) acquisition program. The chromatographic and mass spectrometric conditions were based on the study by Iakovides et al. (2019) with modifications. First, 2μL of the final extract were injected into the GC-MS system using a cool-on-column inlet (50°C constant temperature and 45 mL min $^{-1}$ total flow). The steps of the GC oven temperature protocol were: initial 50°C temperature, hold for 1 min, 30 °C min^{-1} up to 150°C, then 5°C min^{-1} up to 300°C, hold for 20 minutes (54.33 min total run time). The transfer line was kept at 300°C, while the MS quadrupole and source temperature were modified to 150 and 230°C, respectively. Helium was used as carrier gas at a flow of 1 mL min^{-1}.

On the day of the analysis, injections with internal standards were run in order to calculate relative response factors. Each sample was spiked with standard mixture of 16 EPA deuterated PAHs for the calculation of the recovery efficiency.

The PAHs standards were purchased from LGC Standards (Teddington, Middlesex, UK). SupraSolv solvents for gas chromatography n-hexane, dichloromethane, ethyl acetate and acetone were obtained from Merck (Darmstadt, Germany). Finally, silica gel (0.040-0.063mm) was purchased from Sigma-Aldrich Chemie GmbH (Taufkirchen, Germany). All the materials used (silica gel, anhydrous sodium sulphate, glass and cotton wool) were processed with an accelerated solvent extraction system (Dionex ASE 300) with n-hexane - dichloromethane (50:50). Glassware was cleaned at 400ºC overnight and was rinsed with n-hexane before use.

Information of the determined PAH members and their quantification are provided in Table S1.

Table S1: List of detected PAHs

Ion	Name	Abbreviation	Detection Limit (ng m^{-3})	Rings	TEF	Carcinogenic Group (IARC 2018)
128	Naphthalene	Nap	0.042	2	0.001	2B
152	Acenaphthylene	Acy	0.001	3	0.001	-
154	Acenaphthene	Ace	0.001	3	0.001	3
166	Fluorene	Flu	0.003	3	0.001	3
178	Phenanthrene	Phe	0.011	3	0.001	3
192	Methyl-Phenanthrene	C1-Phe	0.007	3	-	-
192	Methyl-Phenanthrene	C1-Phe	0.007	3	-	-
192	Methyl-Phenanthrene	C1-Phe	0.007	3	-	-
192	Methyl-Phenanthrene	C1-Phe	0.007	3	-	-
206	Dimethyl-Phenanthrene	3.6 DMP	0.002	3	-	-
206	Dimethyl-Phenanthrene	2.6 DMP	0.002	3	-	-
206	Dimethyl-Phenanthrene	2.7 DMP	0.002	3	-	-
206	Dimethyl-Phenanthrene	1.3/2.10/3.9/3.10 DMP	0.002	3	-	-
206	Dimethyl-Phenanthrene	1.6/2.9 DMP	0.002	3	-	-
178	Anthracene	Ant	0.002	3	0.01	3
202	Fluoranthene	Flt	0.002	4	0.001	3
202	Pyrene	Pyr	0.003	4	0.001	3
216	Methyl-Fluoranthene/Pyrene	C1-202	0.003	4	-	-
216	Methyl-Fluoranthene/Pyrene	C1-202	0.003	4	-	-
216	Methyl-Fluoranthene/Pyrene	C1-202	0.003	4	-	-
216	Methyl-Fluoranthene/Pyrene	C1-202	0.003	4	-	-
228	Benzo[*a*]anthracene	BaA	0.001	4	0.1	2B
228	Chrysene	Chr	0.002	4	0.01	2B
252	Benzo[*b* & *k*]fluoranthene	BbkF	0.002	5	0.1	2B
252	Benzo[*e*]pyrene	BeP	0.001	5	0.01	3
252	Benzo[*a*]pyrene	BaP	0.001	5	1	1
252	Perylene	Per	0.002	5	0.001	3
276	Indeno[1,2,3-*cd*])pyrene	IP	0.004	6	0.1	2B
276	Anthanthrene	Anth	0.002	6	-	3
278	Dibenzo[*ah*]anthracene	DBahA	0.001	5	1	2A
276	Benzo[*ghi*]perylene	BghiP	0.003	6	0.01	3
300	Coronene	Cor	0.001	7	0.001	3

Section S2. Source apportionment

PMF modeling

PMF modelling (Paatero and Tapper, 1994) and specifically the ME-2 program(Paatero, 1999) as incorporated in the USEPA PMF software (Norris et al., 2014) was applied for identification and apportionment of carbonaceous aerosol sources. In short, the PMF model utilizes chemical speciation data to obtain source contribution times-series and a source profile matrix, minimizing the uncertainty-weighted errors of the chemical mass balance equation, under non-negativity constraints for source contributions. The selection of the optimal number of sources to be resolved by the model is essentially a question of physical interpretation of the sources, model predictive ability and stability of the solution. In the present case, the dataset used consisted of 24-hour averaged samples. The 12-h samples collected during the winter campaigns were integrated for daily periods of 6:00-6:00 LST duration. In total, 104 24-h samples were considered for the analysis. The carbonaceous aerosol speciation dataset consisted of OC and EC, PAHs, oxalate and levoglucosan. Low-MW, highly volatile PAH members (Nap, Acy, Ace, Flu, Phe) were not considered for the analysis since their temperature dependence can artificially bias results and also lead to underestimation of contributions for factors in which they would have a large participation (Wang et al., 2016). Mannosan and galactosan were also excluded to limit redundancy, since they recorded near-perfect correlations ($r > 0.99$) with levoglucosan. Total carbon (TC: sum of OC, EC) was included as a total variable in the PMF model, for a meaningful mass balance approach (Piletic et al., 2013; Valotto et al., 2017)

Uncertainties for each data point (u_{ij}) were calculated as:

$$u_{ij} = \sqrt{DL_j{}^2 + (x_{ij}R_j)^2}$$

where DL_j the detection limit of the species (j), R_j the calculated analytical precision in its determination based on replicate measurements in selected samples and x_{ij} its determined concentration on a sample (i) (Norris et al., 2008).The uncertainty of TC was calculated from uncertainties of its components (OC, EC) under standard rules of uncertainty propagation (square root of sum of squared uncertainties). Uncertainties of samples integrated from two 12-h measurements were calculated in the same way. Data values lower than the respective limits of detection were assigned the 5/6th of the LOD as uncertainty (Polissar et al., 1998). Missing values were substituted with the median concentration and linked to an uncertainty four times the median.

The inclusion of species in the final model was based on their signal to noise (S/N) ratios, with those having S/N values lower than 0.5 (“bad” species) being excluded from the analysis and those with values in 0.5-2 (“weak species”) having their uncertainty tripled (Paatero and Hopke, 2003). The total variable had also its uncertainty tripled. In total, 16 species measured in filter samples were entered in the analysis, including 12 PAH members. Extra modelling uncertainty was included to account for random errors and variations in the source profiles leading to more stable solutions and to ensure standard residuals in the [-3,3] range for the majority of data points in the analysis (Callén et al., 2009). The repeatability of the lowest Q solution was tested using different starting seeds (20 replications). Rotational and random errors were assessed using the bootstrap (BS) and displacement (DISP) error estimation methods included in

the EPA PMF 5.0 software (Paatero et al., 2014). Details on PMF model design parameters are provided in Table S2 below, according to the reporting guidelines of Brown et al. (2015).

Selected PMF solution

PMF solutions with 3-8 factors were examined, with the decrease in Q_{Robust} / $Q_{EXPECTED}$ being gradually halted beyond the first four factors. Moreover, the four-factor solution was deemed the most physically meaningful, given also that factor splitting was observed for solutions with more factors, with additional factors being dominated by single species.

Three of the four factors were attributed to local combustion sources (biomass, gasoline, diesel/oil) and the fourth encompasses non-local/regional sources of carbonaceous aerosol. The selected solution reconstructed well the mass of TC (r: 0.90, slope: 0.88) and Σ-PAHs (r: 0.92, slope: 0.98). It was robust, displaying small rotational and random errors, as assessed by the bootstrap (BS) and displacement (DISP) procedures. Over 90% of 100 bootstrap replications were correctly matched to the initial solutions and no factor swaps were observed. Levoglucosan, as a marker of fresh biomass burning, was dominant since the initial solution (49%) in the respectively identified source. It was constrained in the two other primary combustion sources (pulled down maximally for a dQ of 0.50%), in order to achieve a clearer separation of sources – 86% in the biomass burning source of the constrained solution (Wang et al., 2016). Data on the PMF solution, performance evaluation and uncertainties are also provided in Table S2.

Table S2: Summary of PMF parameters and error estimation (EE) diagnostics

PMF parameters	
Software	EPA PMF 5.0, ME-2, robust mode
Number of included species	16
Number of samples	104
Down-weighted ("weak") species [a]	Flt, Pyr, Levoglucosan
Excluded ("bad") species [b,c]	Nap, Acy, Ace, Flu, Phe, Me-Phe, DMP, Ant, Me-Flt/Pyr, Anth
Total Variable[d]	TC
Added modelling uncertainty	12%
Number of runs	100
Robust mode	Yes
Seed selection	Random
PMF diagnostics – base solution (4 factors)	
Q_{TRUE}	2702.6
Q_{ROBUST}	2664.0
Q_{ROBUST} / Q_{EXP}	2.40
Q_{ROBUST} / Q_{EXP} (-1 factor)	3.04
Q_{ROBUST} / Q_{EXP} (+1 factor)	2.22
Q_{ROBUST} / Q_{EXP} (+2 factor)	1.96
Q_{ROBUST} / Q_{EXP} (+3 factor)	1.89
Q_{ROBUST} / Q_{EXP} (+4 factor)	1.73
PMF diagnostics – constrained solution (final)	
Constrains	Levoglucosan, pulled down maximally, dQ: 0.50%, diesel/oil and gasoline factors
dQ	12.4 (0.47%)
Q_{ROBUST}	2676.5
Species with $Q/Q_{EXP} > 3$	-
Cases with $Q/Q_{EXP} > 3$	3 (2.9%)
r^2	0.82 for TC, 0.84 for Σ-PAHs
Slope [e]	0.88 for TC, 0.98 for Σ-PAHs
Unaccounted fraction	3% for TC, 7% for Σ-PAHs
Error evaluation (bootstrap – BS, displacement – DISP) – constrained solution	
% of BS factors assigned [f]	90% for diesel/oil, 100% for the others
DISP %dQ	-0.002
Species displaced	All non-"weak"
DISP swaps	0

[a] Species with signal to noise ratio (S/N) values between 0.5 - 2. Uncertainty tripled

[b] Species with signal to noise ratio (S/N) values below 0.5 were not included in PMF

[c] 2-3 ring PAHs (Nap-Phe) excluded due to their minor fractionation in the particle phase

[d] Total variable uncertainty tripled

[e] Estimated-to-observed

[f] From 100 bootstrap runs, $r = 0.6$ (default)

Section S3: Temporal Variability of PAH concentrations and controlling factors

Table S3: Studies for PAHs in the Greater Area of Athens (I – continued in the next page)

Sampling period	Number of samples	Sites	PM fraction	BaP average (ng m^{-3})	ΣPAHs average (ng m^{-3})	Reference
02/1984 - 05/1984	43	4 sites (2 Urban Commercial, Urban Industrial, Industrial)	TSP	2.3-5.7	-	Athanasiou et al., 1986
02/1984 - 02/1985	302	4 sites (2 Urban Commercial, Urban Industrial, Industrial)	TSP	2.1-4.0 (BeP + BaP)	13.2-24.2 (9 PAHs)	Viras et al., 1987
02/1984 - 02/1985	172	5 sites (2 Urban Commercial, Urban Industrial, Industrial, Rural Background)	TSP	1.5-4.2 (min:0.1, max:12.5)	-	Viras et al., 1990
02/1984 - 02/1986	650	4 sites (2 Urban-Commercial, Urban Industrial, Industrial)	TSP	1.8-4.0	12.3-24.2 (9 PAHs)	Viras and Siskos, 1993
01/1996 - 12/1996	32	Urban Background	TSP	0.61 (0.18-1.32)	23.9 (9.3-33.8) (8 PAHs)	Marino et al., 2000
12/1997 - 07/1998	19	Urban Traffic	TSP	-	51.1 (4.6 - 278.0) (8 PAHs)	Sitaras and Siskos, 2001
07/2000	9	Urban Background, Suburban Background, Regional Background	TSP	Urban Background: 0.17	Urban Background: 4.94 (20 PAHs)	Mandalakis et al., 2002
05/2001 - 06/2002	186	4 sites (Urban Traffic - ARI, Urban - MAR, Suburban Background -THR, Urban Industrial - ELE)	PM_{10}	MAR: 0.16 (0.01-0.80), ARI: 0.56 (0.03-4.68), ELE: 0.71 (0.02-4.18), THR: 0.04 (0.01-0.24)	MAR: 2.84 (0.19-7.60), ARI: 8.54 (1.80-52.13), ELE: 7.93 (0.60-38.38), THR: 0.66 (0.28-1.93) (13 PAHS)	Mantis et al., 2005
12/2003 - 02/2004, 05/2004 - 07/2004	14	Urban Traffic	TSP, $PM_{10.2}$, $PM_{2.1}$	TSP: 2.89 $PM_{10.2}$: 0.48 $PM_{2.1}$: 0.29	-	Valavanidis et al., 2006
06/2003, 11/2003 - 12/2003	55	2 sites (Suburban Background - S1, S2)	TSP	S1: 0.21 (0.02-1.36) S2: 0.25 (0.02-1.28)	S1: 3.21 (0.44–13.2), S2: 3.08 (0.51-12.7) (14 PAHs)	Vasilakos et al., 2007

Table S3: continued

Sampling period	Number of samples	sites	PM fraction	BaP ng m3 (average)	ΣPAHs ng m3 (average)	Reference
6/2003 - 7/2003	14	Urban Background	Ultrafine ($PM_{0.2}$), accumulation ($PM_{0.2–1}$), intermodal ($PM_{1–2.5}$) and coarse ($PM_{2.5–10}$)	PM_{10}: 0.05, $PM_{2.5}$: 0.05,	PM_{10}: 2.93, $PM_{2.5-10}$: 1.19, $PM_{0.2-2.5}$: 1.46, $PM_{0.2}$: 0.275 (32 PAHs)	Saarnio et al., 2008
08/2003, 03/2004	-	2 sites (Urban Traffic: Athinas, Urban Background: AEDA)	$PM_{2.5}$, $PM_{2.5-10}$	08/2003 Athinas: $PM_{2.5}$: 0.10 03/2004 Athinas: $PM_{2.5}$: 2.05 03/2004 AEDA $PM_{2.5}$: 1.54	08/2003 Athinas: $PM_{2.5}$: 1.17 03/2004 Athinas: $PM_{2.5}$: 28.91 03/2004 AEDA $PM_{2.5}$: 32.61	Andreou and Rapsomanikis, 2009
04/2010 - 04/2011	60	21 sites (7 Urban Traffic, 14 Urban Background)	$PM_{2.5}$	0.25 (0.11−0.76)	2.00 (8 PAHs)	Jedynska et al., 2014
01/2013 - 02/2014	-	Suburban Background	$PM_{2.5}$	Winter: 0.21 (0.10-0.30) Summer: 0.06 (0.05-0.12)	Winter: 3.44, Summer: 0.66 (27 PAHs)	Alves et al., 2017
12/2013 - 02/2014	21	Urban Background	$PM_{2.5}$	3.8 (0.3-13.4)	-	Fourtziou et al., 2017a
11/2013, 09/2014	104	Urban Traffic	PM_{10}, $PM_{2.5}$, PM_1		PM_{10}: 15.80, $PM_{2.5}$: 7.73, PM_1: 7.38 (20 PAHs)	Pateraki et al., 2019
2008	20	3 sites (Suburban Background - site 1), Urban Industrial - site 2) Coastal Background -site 3)	$PM_{2.5}$, PM_1	$PM_{2.5}$: Site 1: 0.02, Site 2: 0.06, Site 3: 0.04 PM_1: Site 2: 0.04, Site 3: 0.004	$PM_{2.5}$: Site 1: 0.43, Site 2: 1.56, Site 3: 0.93 PM_1: Site 2: 0.90, Site 3: 0.21 (20 PAHs)	Pateraki et al., 2019
12/2018 - 02/2019, 5/2019-7/2019	30	Urban Industrial	PM_{10}	Total: 0.93 (0.04-3.07), Cold period: 1.03 (0.23-2.34), Warm period: 0.57 (0.04-3.07)	Total: 7.07 (1.27-16.50), Cold period: 8.44 (2.88-16.50), Warm period: 2.01 (1.27-4.46) (15 PAHs)	Koukoulakis et al., 2020
06/2018 – 05/2019	56	Urban Industrial	PM_{10}	Total: 1.4, Summer: 0.09, Autumn: 3.6, Winter: 1.7, Spring: 0.43	Total: 9.8, Summer: 0.60, Autumn: 20.6, Winter: 13.0, Spring: 5.0 (13 PAHs)	Kanellopoulos et al., 2021
12/2016 - 01/2018	***156***	***Urban Background***	***$PM_{2.5}$***	***Total: 0.44, Winter: 0.81, Spring: 0.02, Summer: 0.04, Autumn: 0.10***	***Total: 7.64, Winter: 13.48, Spring: 2.53, Summer: 0.89, Autumn: 2.19 (31 PAHs)***	***This study***

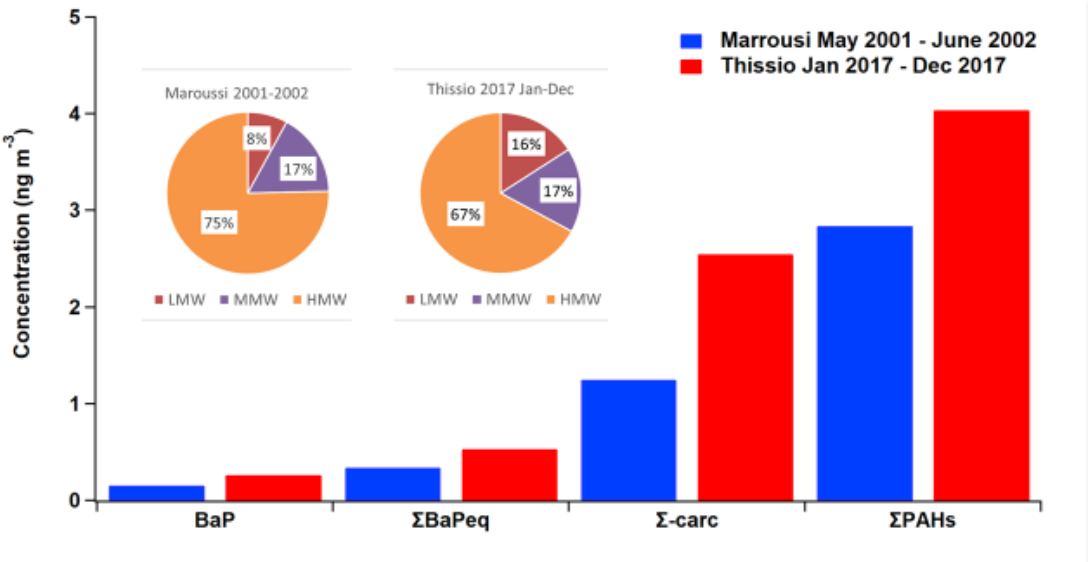

Figure S2: Comparison of results from the present study (for the calendar year of 2017 at Thissio, Athens), with results from a yearlong study 15 years earlier, preceding the Greek economic recession (June 2001 – May 2002, at Maroussi, Athens). Both sites are located more than 300m from major roads. Displaying results for BaP, BaPeq, the sum of carcinogenic PAHs (Σ-carc) and Σ-PAHs (Mantis et al., 2005).

Table S4: Seasonal variability of PAH levels (winter vs. non-winter measurements) and *p*-values for statistical significance of mean differences (t-test, assuming non-equal variances). Winter corresponds to the December 2016 – February 2017 and December 2017 – January 2018 periods.

Name	Season	Mean	p
Nap	Winter	0.59	<0.01
	Non-Winter	0.12	<0.01
Acy	Winter	0.06	<0.01
	Non-Winter	0.02	<0.01
Ace	Winter	0.08	<0.01
	Non-Winter	0.01	<0.01
Flu	Winter	0.11	<0.01
	Non-Winter	0.03	<0.01
Phe	Winter	0.43	<0.01
	Non-Winter	0.11	<0.01
Σ C1-Phe	Winter	0.02	0.02
	Non-Winter	0.01	0.02
Σ DMP	Winter	0.08	<0.01
	Non-Winter	0.02	<0.01
Ant	Winter	0.09	<0.01
	Non-Winter	0.01	<0.01
Flt	Winter	0.36	<0.01
	Non-Winter	0.10	<0.01
Pyr	Winter	0.39	<0.01
	Non-Winter	0.12	<0.01
Σ C1-202	Winter	0.15	0.06
	Non-Winter	0.00	0.06
BaA	Winter	0.60	<0.01
	Non-Winter	0.02	<0.01
Chr	Winter	0.99	<0.01
	Non-Winter	0.04	<0.01
BbkF	Winter	3.39	<0.01
	Non-Winter	0.29	<0.01
BeP	Winter	0.97	<0.01
	Non-Winter	0.07	<0.01
BaP	Winter	0.82	<0.01
	Non-Winter	0.05	<0.01
Per	Winter	0.25	<0.01
	Non-Winter	0.01	<0.01
IP	Winter	1.40	<0.01
	Non-Winter	0.11	<0.01
Anth	Winter	1.02	<0.01
	Non-Winter	0.04	<0.01
DBahA	Winter	0.17	<0.01
	Non-Winter	0.01	<0.01
BghiP	Winter	1.30	<0.01
	Non-Winter	0.10	<0.01
Cor	Winter	0.35	<0.01
	Non-Winter	0.03	<0.01

Partitioning

The estimation of PAHs partitioning between gas and particulate phase was made based on the partitioning theory of semi-volatile organics due to absorption by organic material in the particle phase (Pankow, 1994). Many studies on PAHs had used the same method (e.g Andreou and Rapsomanikis, 2009; Xie et al., 2013). The gas/particle concentration ratios are calculated through the partitioning-absorption equations and the calculation of the partitioning coefficient $K_{p.}$

$$k_{P,OM} = \frac{P}{G\ M_{OM}}$$

$$k_{P,OM} = \frac{RT}{10^6 \overline{MW_{OM}}\ \zeta_{OM}\ p_L{}^0}$$

where $k_{P,OM}$ is the coefficient of partitioning ($m^3\ \mu g^{-1}$) to the absorbing organic aerosol material (OM), G and P the mass fractions of each PAH in the gas and particle phase, respectively (ng m^{-3}), M_{OM} is the mass concentration of particle-phase OM (ng m^{-3}), $\overline{MW_{OM}}$ the average molecular weight of OM, ζ_{OM} is the activity coefficient of each PAH in the absorbing OM phase and $p_L{}^0$ (atm) is the vapor pressure of each pure PAH compound in the ambient temperature of interest.

For M_{OM} concentrations we used the ACSM-measured OA, and – where data were missing – we inserted the measured OC concentrations multiplied by an OA/OC factor of 1.6, that has been shown to be representative in the sampling site (Stavroulas et al., 2019) An average MW_{OM} of 200 g mol^{-1} was set, in accordance with relevant studies for urban sites (Williams et al., 2010; Xie et al., 2013). Various studies have reported mean MW in the range of 270-340 g mol^{-1} for highly processed OM (Romonosky et al., 2016; Vogel et al., 2016) and consequently we consider 200 g mol^{-1} to be a reasonable approximation at our site where there is a substantial fraction of primary and less processed OM year-round (Stavroulas et al., 2019).

For the calculation of $p_L{}^0$ the following equation was used:

$$p_L{}^0 = p_L{}^{0*}\ exp\left[\frac{\Delta H_{vap}{}^*}{R}\left(\frac{1}{298.15} - \frac{1}{T}\right)\right]$$

where $p_L{}^{0*}$ is the vapor pressure of each PAH at 25ºC, $\Delta H_{vap}{}^*$ is its vaporization enthalpy as a liquid, and T is the average temperature during each sample's duration. The values of the two thermochemical parameters were retrieved from published databases in scientific review articles (Achten and Andersson, 2015; Roux et al., 2008).

The results indicate that, as expected, the largest fractions of LMW PAHs are partitioned in the gas phase (71% - 100%). Most MMW and all HMW PAHs are partitioned preferentially in the particle phase, at rates ranging between 90%-100%, with the exception of the lighter Flt and Pyr. The results support the decision not to include the LMW PAH members in the source apportionment analysis, since their temperature-dependent partitioning could induce large uncertainties in the source-receptor relationships. It also appears that it was indeed useful to downweight the involvement in the PMF model of Flt and Pyr (15%, 25% in the particle phase).

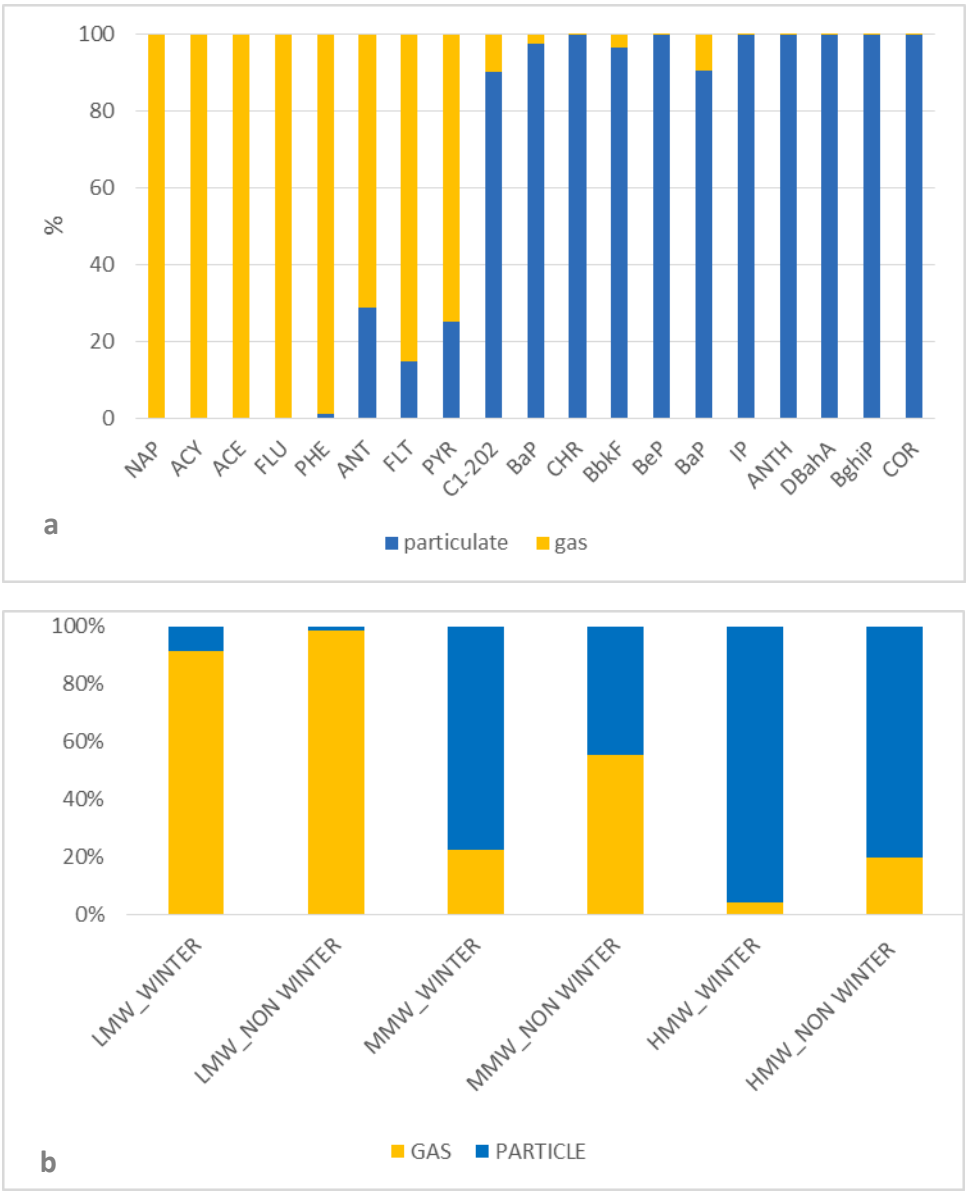

Figure S3: Gas-Particle Fractions (a) in PAH members for the entire sampling season and (b) in LMW, MMW and HMW PAHs in winter and non-winter season.

Table S5: Correlations of PAHS with O_3, NO_x and CO concentrations. UB signifies the Thissio urban background site, TR the traffic Athinas Str. site of the regulatory air quality monitoring network (0.9 km to the NE of Thissio).

	Full Period				Winter				Non-Winter			
PAHs	NOx - UB (N=104)	NOx - TR (N=97)	CO - UB (N=134)	O_3 - UB (N=133)	NOx - UB (N=41)	NOx - TR (N=65)	CO - UB (N=71)	O_3 - UB (N=70)	NOx - UB (N=63)	NOx - TR (N=32)	CO - UB (N=63)	O3 - UB (N=63)
NAP	0.18	**0.40**	**0.35**	**-0.33**	0.18	**0.36**	0.23	-0.15	0.03	-0.01	0.07	-0.12
ACY	0.20	**0.56**	**0.47**	**-0.39**	0.28	**0.54**	**0.40**	**-0.32**	-0.08	-0.25	-0.09	-0.02
ACE	0.20	**0.37**	**0.31**	**-0.32**	0.24	**0.33**	0.19	-0.15	-0.04	-0.13	-0.01	-0.11
FLU	0.21	**0.34**	**0.30**	**-0.30**	0.36	0.29	0.20	-0.15	-0.08	-0.04	-0.05	0.02
PHE	0.18	0.18	0.21	**-0.25**	0.13	0.06	0.02	0.05	0.02	0.17	0.06	0.03
Σ C-Phe	0.20	0.01	0.09	-0.18	0.08	-0.05	-0.04	0.04	**0.45**	**0.66**	**0.49**	**-0.51**
Σ DMP	**0.28**	**0.42**	**0.35**	**-0.31**	0.24	**0.40**	0.26	-0.14	0.26	0.20	0.31	**-0.35**
ANT	**0.30**	**0.43**	**0.40**	**-0.37**	0.32	**0.39**	0.29	-0.24	0.21	0.10	0.25	-0.30
FLT	0.09	0.26	**0.29**	**-0.35**	0.04	0.10	0.07	-0.11	-0.16	0.27	-0.10	0.20
PYR	0.05	**0.50**	**0.41**	**-0.34**	0.14	**0.40**	**0.37**	**-0.33**	-0.23	0.43	-0.16	0.29
C1-202	**0.45**	**0.83**	**0.69**	**-0.41**	**0.56**	**0.83**	**0.70**	**-0.51**	**0.39**	**0.53**	**0.55**	**-0.49**
BaP	0.12	**0.78**	**0.69**	**-0.43**	0.06	**0.78**	**0.67**	**-0.45**	0.23	**0.50**	**0.40**	**-0.35**
CHR	**0.52**	**0.83**	**0.81**	**-0.50**	**0.63**	**0.82**	**0.82**	**-0.60**	0.32	**0.49**	**0.49**	**-0.46**
BbkF	**0.58**	**0.88**	**0.86**	**-0.59**	**0.72**	**0.87**	**0.86**	**-0.69**	0.29	**0.51**	**0.47**	**-0.33**
BeP	**0.56**	**0.86**	**0.85**	**-0.55**	**0.63**	**0.85**	**0.85**	**-0.64**	**0.46**	**0.59**	**0.63**	**-0.57**
BaP	**0.37**	**0.81**	**0.81**	**-0.47**	**0.64**	**0.81**	**0.84**	**-0.59**	-0.01	**0.48**	0.08	0.05
PER	**0.29**	**0.83**	**0.81**	**-0.49**	0.31	**0.82**	**0.82**	**-0.57**	-0.04	0.36	0.11	-0.07
IP	**0.57**	**0.88**	**0.83**	**-0.59**	**0.67**	**0.87**	**0.82**	**-0.67**	**0.36**	**0.59**	**0.55**	**-0.49**
ANTH	0.24	**0.77**	**0.68**	**-0.50**	0.20	**0.75**	**0.62**	**-0.46**	**0.37**	**0.58**	**0.56**	**-0.45**
DBahA	**0.30**	**0.70**	**0.73**	**-0.51**	0.34	**0.68**	**0.69**	**-0.55**	0.14	**0.47**	0.29	**-0.35**
BghiP	**0.41**	**0.89**	**0.87**	**-0.62**	**0.40**	**0.88**	**0.86**	**-0.69**	**0.46**	**0.65**	**0.63**	**-0.57**
COR	**0.59**	**0.86**	**0.75**	**-0.52**	**0.64**	**0.86**	**0.74**	**-0.63**	**0.68**	**0.73**	**0.81**	**-0.73**

Section S4: Investigating intense pollution events: nighttime vs. daytime

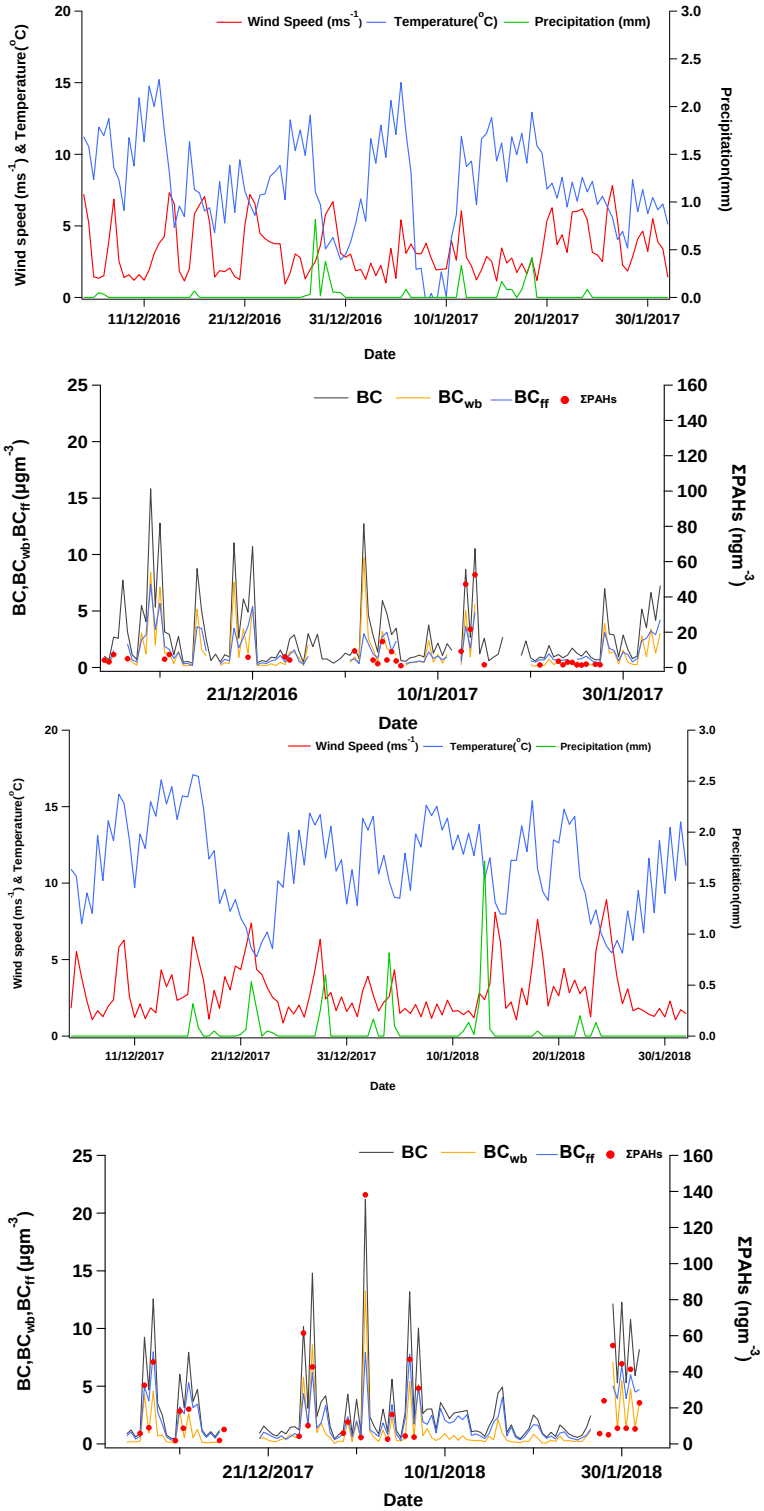

Figure S4: Temporal variability of meteorological parameters (1-hour values, left) and BC-ΣPAHs (right) during the two winter periods (2016-2017: upper panels, 2017-2018: lower panels).

Table S6: Pearson correlations (r and statistical significance p) between ΣPAHs and other tracers, for nighttime and daytime winter samples, during intense pollution events (IPE)

	IPE SAMPLES					
	DAY			NIGHT		
	r	***p***	**Number**	***r***	***p***	**Number**
nss-K^{+} ***	0.13	0.58	20	0.81**	<0.01	30
BC	0.10	0.70	18	0.92**	<0.01	28
BC_{bb}	0.20	0.43	18	0.95**	<0.01	27
BC_{ff}	0.04	0.88	18	0.81**	<0.01	25
BC_{bb} vs nssK^{+}	*0.35*	*0.16*	*18*	*0.72***	*<0.01*	*27*
nssK vs Levoglucosan***	*0.83***	*<0.01*	*10*	*0.84***	*<0.01*	*17*
nssK vs Mannosan***	*0.84***	*<0.01*	*10*	*0.86***	*<0.01*	*17*
nssK vs Galactosan***	***0.71*****	*<0.01*	*10*	*0.83***	*<0.01*	*17*
OC	0.38	0.10	20	0.92**	<0.01	30
EC	0.14	0.56	20	0.53**	<0.01	30
Levoglucosan	0.87**	<0.01	10	0.93**	<0.01	17
Mannosan	0.89**	<0.01	10	0.93**	<0.01	17
Galactosan	0.75**	<0.01	10	0.90**	<0.01	17
m/z 60	0.14	0.55	20	0.88**	<0.01	30
m/z 73	0.07	0.78	20	0.86**	<0.01	30
OA	0.17	0.48	20	0.90**	<0.01	30
HOA	-0.08	0.83	10	0.80**	<0.01	13
BBOA	0.20	0.59	10	0.93**	<0.01	13
COA	-0.37	0.29	10	0.55*	0.05	13
SV-OOA	0.02	0.95	10	0.90**	<0.01	13
LV-OOA	-0.06	0.87	10	-0.15	0.62	13
SO_4^{2-} ***	0.09	0.72	20	0.24	0.21	29
NO_3^{-}***	-0.05	0.83	20	0.31	0.10	30

100

* Correlation statistically significant at the 0.05 level

**Correlation statistically significant at the 0.01 level

***From filter analysis

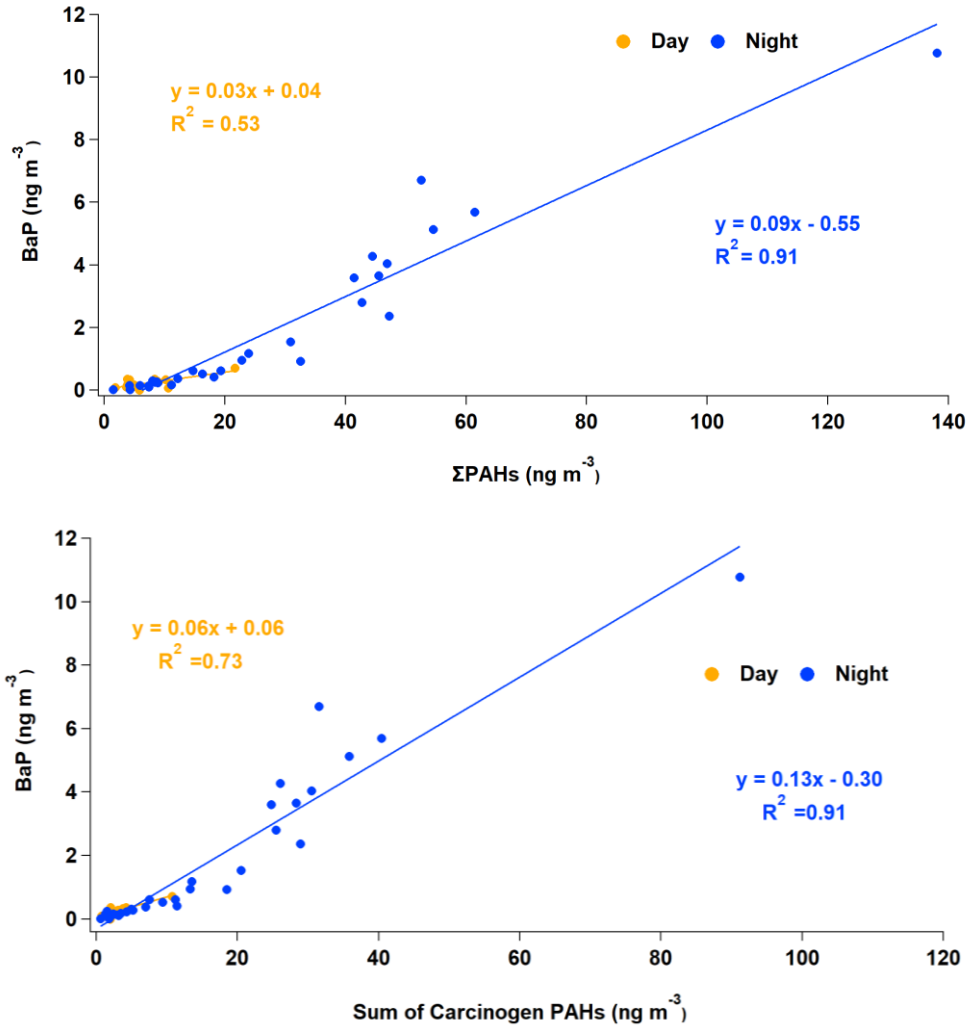

Figure S5: Scatterplot of BaP with sum of carcinogenic PAHs (upper panel) and Σ-PAHs (lower panel), during the IPE days (yellow) and nights (blue).

Table S7: Concentration ± standard deviation (µg m^{-3}) and diagnostic ratios of monosaccharide anhydrides during intense pollution events (IPE).

	IPE day	IPE night
Levoglucosan	0.27 ± 0.13	2.79 ± 2.03
Mannosan	0.03 ± 0.01	0.34 ± 0.26
Galactosan	0.01 ± 0.01	0.14 ± 0.11
Levoglucosan/Mannosan	8.35 ± 0.56	8.22 ± 0.58
Mannosan/Galactosan	2.64 ± 0.53	2.46 ± 0.21
ΣPAHs (ng m^{-3})/Levoglucosan (µg m^{-3})	30.27 ±11.31	14.25 ± 3.43
Levoglucosan/(Mannosan + Galactosan)	6.01 ± 0.44	5.83 ± 0.48

115

Section S5: PMF source characterization

The contribution profiles of the four sources are provided in Figure 2. Bivariate polar plots of source contributions to Σ-PAHs depending on wind speed and direction are presented in Figure S6 and a comparison of standardized mean contributions between winter/non-winter months in Figure S7.

Characterization of identified sources

Local combustion-related sources (biomass, gasoline, diesel/oil)

- Statistical significant correlations with external combustion tracers (BC_{ff}, BC_{bb}, CO).
- BaA/(BaA+Chr) diagnostic ratios (DR) over 0.35, indicative of pyrogenic origin. IP/(IP+BghiP) DR over 0.20, indicative of pyrogenic origin (Katsoyiannis et al., 2011).
- Significantly higher ($p < 0.01$) contributions during the winter months (December – February) compared to the rest of the year (Figure S7), reflecting known seasonal patterns of residential heating and vehicular traffic at the Thissio urban background site, combined with a shallower winter boundary layer (Stavroulas et al., 2019; Liakakou et al., 2020).

Biomass Burning

- High loadings in levoglucosan, a key BB marker.
- Important loadings in 5-6 ring PAHs (Taghvaee et al., 2018; Masiol et al., 2020).
- High loadings in BaA, Chr, BbkF, BaP, Per(Srivastava et al., 2018; Li et al., 2018).
- Strong presence of BaP in the factor consistent with past findings at Thissio reporting direct associations between wintertime BaP levels and several BB tracers (Fourtziou et al., 2017).
- A recent $PM_{2.5}$ source apportionment study in Athens showed a $PM_{2.5}$ BB source profile to be dominated by MMW and HMW PAHs, including BaP, BaA, Chr, IP (Pateraki et al., 2019).
- Notable BB contributions to BaA, Chr, BaP and DBahA reported in Thessaloniki, Greece, by chemical mass balance (CMB) source apportionment (Manoli et al., 2016).
- An important impact of BB on DBahA reported in Thessaloniki, Greece, where average urban background concentrations increased by 20 times between the winters of 2012 and 2013, due to dramatically enhanced residential wood burning (Saffari et al., 2013).
- The highest IP/(IP+BghiP) DR among sources, with a value exceeding 0.5 (0.57), indicative of solid fuel combustion (Dvorská et al., 2011; Lin et al., 2015).
- The only oner of the four sources with an Flt/(Flt+Pyr) ratio higher than 0.5 (0.60), which also suggests wood burning emissions (Yunker et al., 2002).
- OC/EC ratio of 4.2 in the source profile, higher than for the petroleum-related sources, characteristic of fresh BB emissions and comparable to the value (3.7) calculated for the BB source at the same site by a long-term $PM_{2.5}$ source apportionment study (Theodosi et al., 2018a).
- The highest correlations among sources with external BB tracers (BC_{bb}: $r = 0.93$; $nssK^+$: $r = 0.61$, *m/z* 60: 0.88; *m/z* 73: 0.86).

- Strong correlation (r = 0.85) with the BBOA component estimated from PMF analysis in the ACSM data.
- Uncorrelated with BC_{ff} and CO during the non-winter months.
- The polar plot for source contributions (Figure S6) indicate its local character, with an enhancement of concentrations for low-wind conditions, as it has been observed at the same site for fresh BB aerosols emitted in central Athens (Stavroulas et al., 2019; Kaskaoutis et al., 2021).
- Factor present almost exclusively during the winter months (Figure S7), when local wood-burning emissions for residential heating intensify.

Gasoline Vehicles

- Stronger contributions to HMW PAHs, such as IP, BghiP and Cor, in comparison with lower-MW members, a feature frequently used to differentiate the gasoline source from general traffic sources (Sofowote et al., 2008).
- Most of the PAH content in gasoline exhaust is formed by pyrosynthesis, as opposed to diesel exhaust where the unburnt fuel/lubricant content in PAHs is much more important. The difference mainly emerges due to the relatively lower content of HMW (IP, BghiP, Cor) in diesel lubricating oils (Valotto et al., 2017; Zielinska et al., 2004).
- Similar pattern in the gasoline source profile reported in Thessaloniki, Greece (Manoli et al., 2016) where, as in Athens, the vehicular fleet is dominated by gasoline-powered vehicles.
- OC/EC ratio of 1.9 in the source profile, within the range (1.7-2.3) typically reported for fresh emissions from gasoline vehicles (Grivas et al., 2012).
- Coronene, which is mostly classified in this factor, has been considered as a potential tracer of gasoline exhaust (Ravindra et al., 2008). However, it has been suggested (Shen et al., 2014) that it is a BaP/COR ratio lower than 0.5 (such as the one observed in our case) that could differentiate gasoline emissions from other combustion sources.
- The highest correlations with BC_{ff} (r = 0.79), which on a long-term basis functions mostly as a proxy of traffic emissions impacting Thissio (Liakakou et al., 2020).
- The only factor that recorded statistically significant correlations with CO (r = 0.80) during the non-winter months.
- The absence of strong directional patterns in the polar plot in Figure S6 suggests that the factor is mostly representative of aerosols produced by passenger vehicles in the vicinity of the site (central Athens).
- Higher source contributions observed during the winter months (Figure S7), indicative of increased traffic in the center of Athens (especially during the December holiday period), against notably reduced traffic affecting Thissio in July-August.

Diesel/Oil Combustion

- Characterized by increased abundance of lower MW members (Shirmohammadi et al., 2016; Zheng et al., 2017) compared to the gasoline vehicles source.

- Recorded the highest contributions to Flt and Pyr among local sources and also substantial loadings in BaA, CHR, BbkF and BaP, along with smaller – compared to the gasoline vehicles source– loadings in IP, BghiP (Park et al., 2011; Wang et al., 2020).
- The association of diesel emissions with Flt, Pyr, BaA, BbkF, BaP has been reported by factor analysis studies in other Greek cities (Manoli et al., 2002; Iakovides et al., 2019).
- BaP/(BaP+Chr) DR lower than 0.5 (0.44) in the source profile supports the association of the source with diesel emissions (Cerqueira and Matos, 2019).
- A higher Flt/(Flt+Pyr) DR for diesel/oil combustion compared to the gasoline source (0.45 vs. 0.35 in the present case) has been considered (Mantis et al., 2005) to distinguish the two sources in the GAA.
- OC/EC ratio was 1.6, higher than typically reported values for diesel exhaust, which could indicate moderate aging. Higher OC/EC ratios can be expected also in the cases of HDDV in creeping mode (Pio et al., 2010) and non-traffic oil combustion emissions (e.g. ships in the port).
- Based on the polar plot, this primary factor presents an enhancement for moderate winds of the S-W sector (Figure S6), where primary pollution hot-spots are found (port of Piraeus, the industrial/commercial hub of Athens, the heavily trafficked E75 international route (Grivas et al., 2019). Therefore, the area to the S-W of the site is characterized by increased circulation of light- and heavy-duty diesel vehicles.
- Participation of non-traffic sources in the factor can't be excluded (use of diesel for residential heating or port emissions from oil combustion). Several studies reported similar PMF-extracted factors that combine emissions from diesel vehicles and combustion of heavier oil products (Khan et al., 2015; Han et al., 2018; Sulong et al., 2019). Nevertheless, vehicular emissions are expected to be the primary contributor here, given also a high BghiP/BaP ratio (2.13), a feature that has been used in Athens (Andreou and Rapsomanikis, 2009) to distinguish vehicular from heating diesel emissions.
- Statistically significant ($p < 0.01$) correlations with external combustion indicators, albeit weaker compared to the gasoline source ($r = 0.66$ with CO, $r = 0.39$ with BC_{ff}). Strongly correlated with HOA/CO ($r = 0.74$).

Non-local sources

- High loadings in OC, EC, which at urban background locations are moderately impacted from local primary sources and mostly driven by aerosols transported to the receptor site at a regional scale (Buzcu-Guven et al., 2007; Hasheminassab et al., 2014).
- The prevalence of regionally transported/secondary fine aerosols has been reported by the majority of aerosol source apportionment studies at urban and suburban background sites in the GAA (Paraskevopoulou et al., 2015; Diapouli et al., 2017; Grivas et al., 2018; Theodosi et al., 2018).
- High contribution to oxalate, an important secondary constituent of water-soluble organic carbon (Myriokefalitakis et al., 2011).

- Significant correlations with sulfate and ammonium (r: 0.57 and 0.51, respectively), indicators of regionally-transported secondary aerosol at Thissio (Theodosi et al., 2018).
- Significant correlations with LV-OOA (r = 0.77 and 0.48, during the non-winter months, respectively) and with SV-OOA (r = 0.55 during winter).
- The only factor that showed a statistically significant ($p < 0.01$) enhancement (Figure S7) during the non-winter months.
- The polar plot (Figure S6) displays the typically observed[34] large dispersion of concentration enhancements along the SW-NE axis of the Athens basin, indicating the association of the factor with transport on a larger-than-urban spatial level.
- Considerable loadings of the lighter 4-ring members (Flt and Pyr). Similarly, a $PM_{2.5}$ source apportionment study at a traffic in Athens (Pateraki et al., 2019), in central Athens classified FA and PY separately from heavier PAHs, in a PMF factor dominated by OC and EC.
- Studies performed at regional background sites attributed increased contributions to Flt and Pyr to distant of coal and heavy combustion sources (Wang et al., 2014; Mao et al., 2018; Lhotka et al., 2019; Miura et al., 2019).
- OC/EC ratio of 2.9 in the source profile, increased compared with the diesel/oil and gasoline sources.

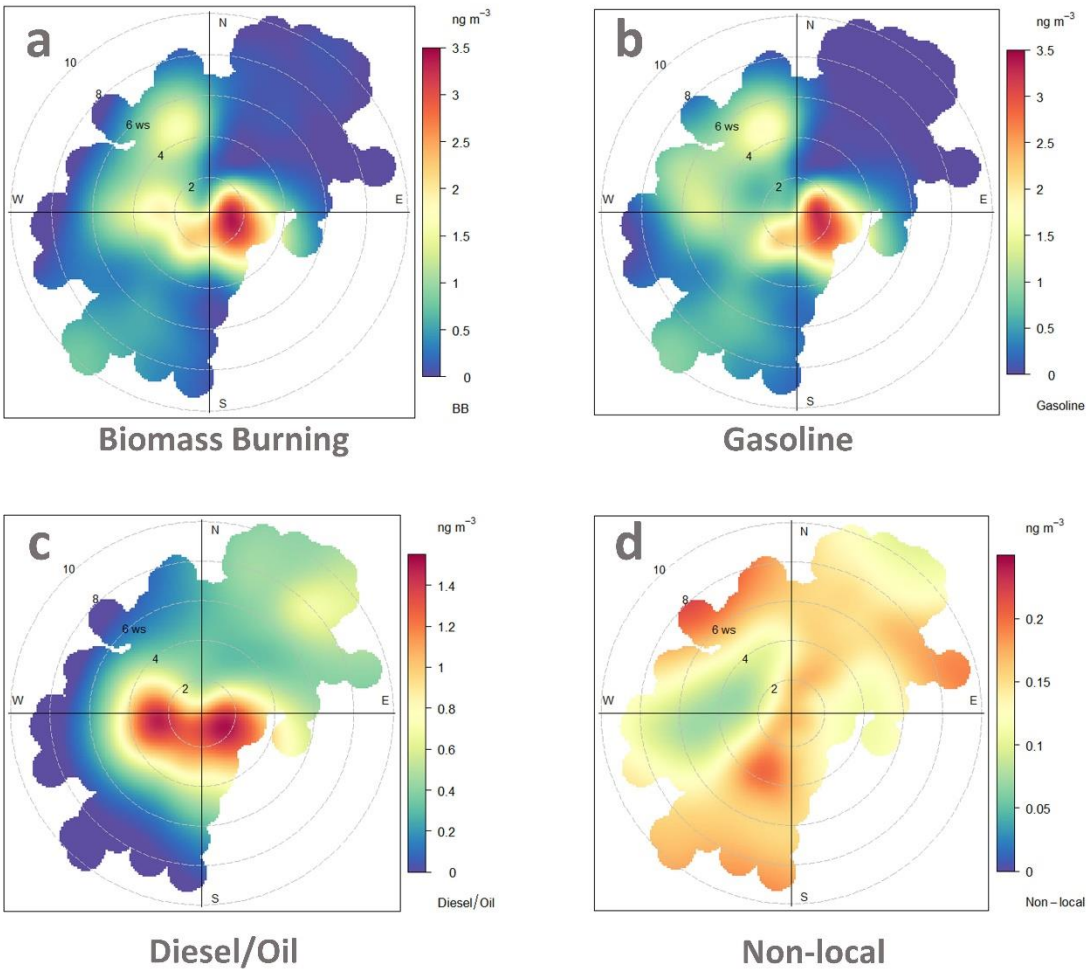

250

Figure S6: Bivariate polar wind plots (wind speed – wind direction) for contributions of identified sources (a-d) to Σ-PAHs concentrations (ng m^{-3}). Wind speed on the radial axis.

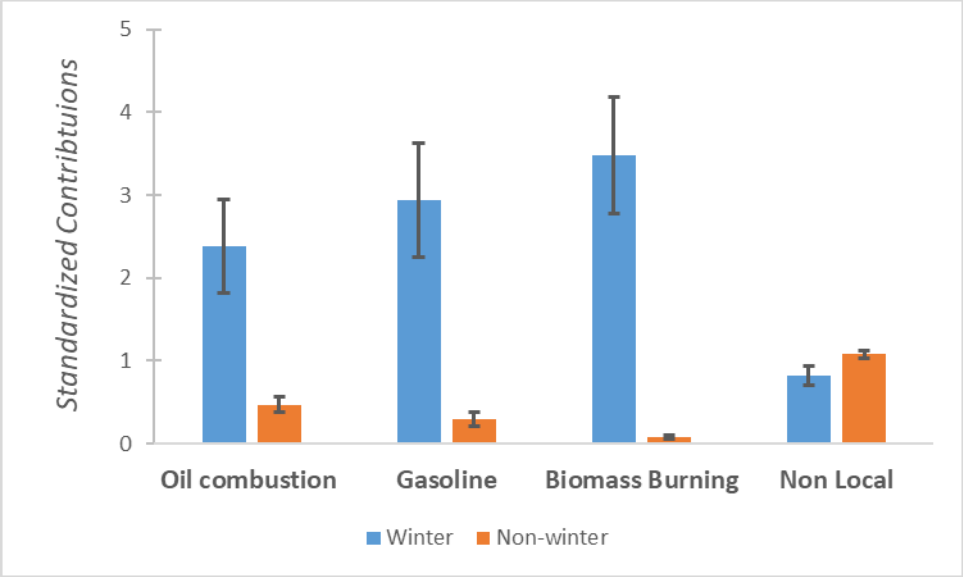

Figure S7: Standardized contributions (± standard error) of PMF-extracted factors, averaged for winter (Dec.-Feb.) and non-winter months of the study period.

Source Contributions to Total Carbon (TC)

Regarding contributions to total carbon, non-local sources were prevalent (65%) at the urban background sampling site (Figure 4a). Similarly, a two-year PMF study at the same site found sources other than traffic and biomass burning to contribute 44% of TC (Theodosi et al., 2018). Moreover, an organic aerosol source apportionment study at Thissio using ACSM measurements (Stavroulas et al., 2019b) reported semi-volatile and low-volatility oxygenated components to dominate total organic aerosol during both the cold (60%) and warm (82%) periods of the year at Thissio. Elsewhere, a study in the Cleveland, OH, area (Piletic et al., 2013), using a PMF model based on organic species including PAHs, found 50-54% of TC to be associated with secondary aerosol. There have been several studies – using receptor modelling, tracer-based or radiocarbon approaches – for source apportionment of carbonaceous aerosols, that report contributions from both local and non-local sources, considerably dependent on seasonal characteristics and site type (Lee et al., 2008; Zhang et al., 2015; Bernardoni et al., 2013). Regarding PMF source apportionment studies, in their majority they have recognized secondary processing and transport of anthropogenic particles on a regional scale to be a major contributor to fine aerosols at urban background locations (Karagulian et al., 2015). However, this pattern frequently doesn't translate also to TC contributions calculated with the same approach, since in the absence of specific organic tracers, OC and EC are usually used as indicators of vehicular traffic (Amato et al., 2016; Saraga et al., 2021). Therefore, results sometimes are contrasting with alternative approaches such as chemical mass balance or tracer methods, that as an example apportion large secondary organic aerosol fractions at background locations (Srivastava et al., 2018).

Local sources here, accounted for a combined 35% of the apportioned TC at the urban background Thissio site, that is generally comparable with results at same site obtained using different chemometric approaches (Stavroulas et al., 2019; Theodosi et al., 2018; Kaskaoutis et al., 2020). It is noted that the mean annual contribution of BB to OC (15%) is comparable to that of the winter BBOA+SV-OOA sum to mean OA, adjusted for the full period (20%). However, the contribution of BB to EC (10%) is less than what would be expected if the mean annual BC_{bb} fraction at the Thissio site was considered (28%), which should be attributed to differences between EC and BC, differences between the two estimations based on chemical and optical properties and also to the fact that the aethalometer model doesn't distinguish between local and non-local sources.

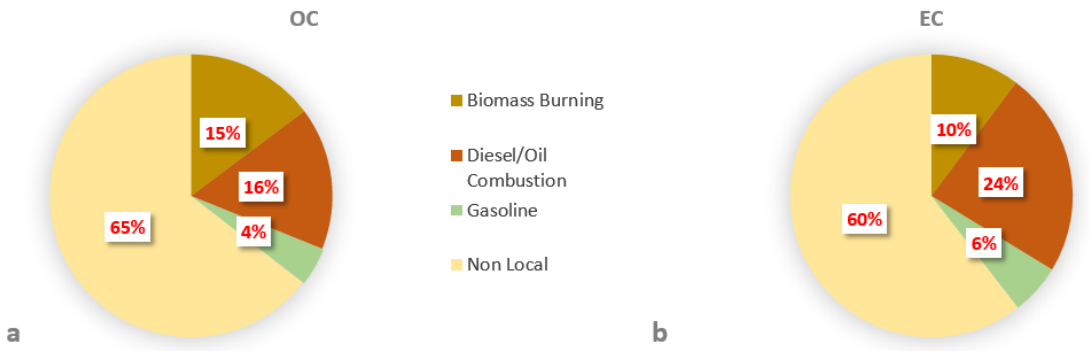

295 **Figure S8: Fractional contributions of PMF-resolved sources to mean modeled concentrations of: a) OC, b) EC**

Section S6: ***Satellite fire maps***

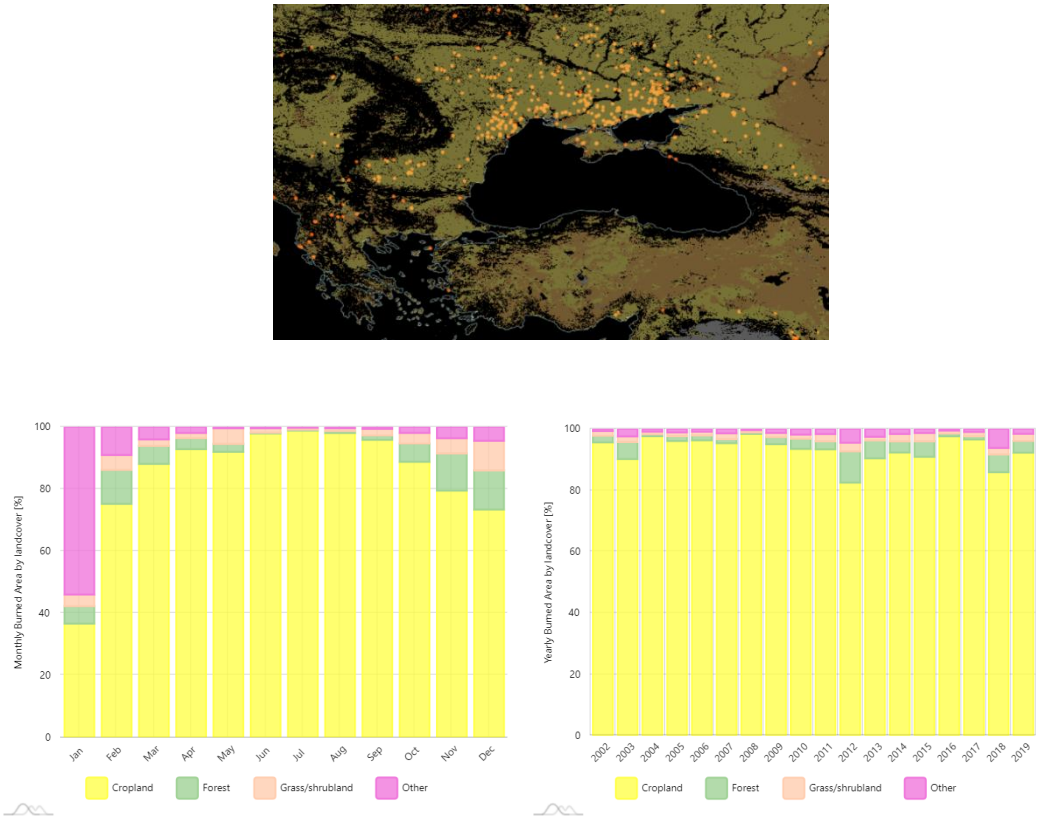

Figure S9: Indicative satellite image (MODIS) on a day in July 2017, showing active fires (light yellow background indicating croplands, according to land cover satellite data) in the Black Sea region (a); average burned area by land cover type in Ukraine during 2002-2019, by month (b) and year (c).

Section S7: Contribution to carcinogenic potency

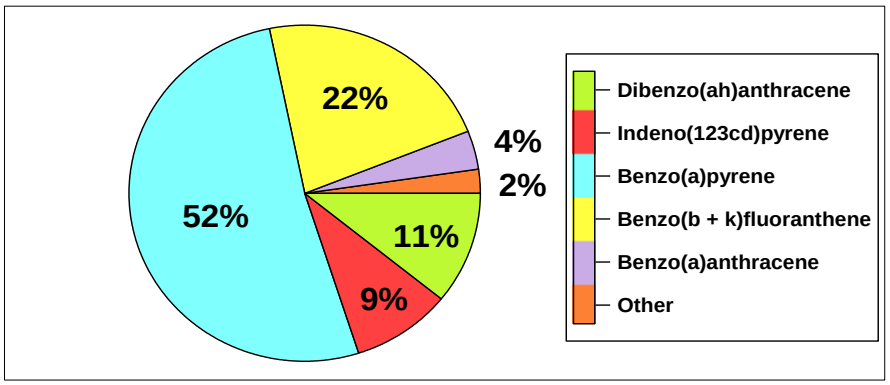

Figure S10: Fraction of estimated BaPeq attributed to various PAH members

320

Table S8: BaPeq values reported at urban sites worldwide

Sampling site	BaPeq (ng m^{-3})	Sampling period	Location	Reference
Athens, Greece	*0.85*	12/2016-01/2018	Urban background	*This study*
Heraklion, Greece	0.06	04/2012 - 02/2014	Urban background	Iakovides et al., 2019
Limassol, Cyprus	0.06	01/2012 - 06/2013	Urban	Iakovides et al., 2019
Madrid, Spain	0.12-0.10	Winter & Summer 2009	Urban background	Mirante et al., 2013
Katowice, Poland	5.3 - 18.5	09/2009-12/2010	Urban background	Kozielska et al., 2014
Venice-Mestre, Italy	1.9	2009 - 2010	Urban background	Masiol et al., 2012
Brno, Czech Republic	0.45-8.7	Winter & Summer 2009 Winter & Summer 2010	Urban	Křůmal et al., 2013
Hamilton, Canada	0.77	Winter & Summer 2009	Intraurban	Anastasopoulos et al., 2012
Khar–Mumbai, India	19	03-05/2007 10-11/2007 12/2007-01/2008	Residential	Abba et al., 2012
Lhasa, Tibet, China	6.3	04/2013 - 03/2014	-	Chen et al., 2018
Lanzhou, China	22-30	Winter & summer 2013	Residential	Wang et al., 2017
Hailun, China	8.3	10/2012 -09/2013	Suburban	Yu et al., 2020
Xi'an, China	2.0 - 64	07/2008- 09/2009	Urban	Bandowe et al., 2014
New York, NY, USA	0.45	10/2005-05/2009	Residential	Jung et al., 2010
10 EPA Regions USA	2.5-3.0	1990-2014	Rural-Urban	Liu et al., 2017

Table S9: Calculated values of BaPeq by season, and associated excess cancer risks, using the two estimation methods (Cal EPA OEHHA, WHO)

	ΣPAHs (ng m^{-3})	***BaP (ng m^{-3})***	***BaPeq (ng m^{-3})***	***ECR OEHHA (x10^{-6})***	***ECR WHO (x10^{-6})***	***% seasonal contribution to ECR***
Jan-Dec 2017	5.22 ± 10.33	0.26 ± 0.89	0.53	0.58	45.73	
Winter	13.5 ± 20.4	0.81 ± 1.78	1.56	0.44	34.59	76
Spring	2.53 ± 4.13	0.02 ± 0.03	0.09	0.03	2.62	6
Summer	0.89 ± 0.87	0.04 ± 0.15	0.07	0.03	1.99	4
Fall	2.19 ± 3.17	0.10 ± 0.20	0.21	0.08	6.52	14

References

Abba, E. J., Unnikrishnan, S., Kumar, R., Yeole, B. and Chowdhury, Z.: Fine aerosol and PAH carcinogenicity estimation in outdoor environment of Mumbai City, India, Int. J. Environ. Health Res., 22(2), 134–149, doi:10.1080/09603123.2011.613112, 2012.

Achten, C. and Andersson, J. T.: Overview of Polycyclic Aromatic Compounds (PAC), Polycycl. Aromat. Compd., 35(2–4), 177–186, doi:10.1080/10406638.2014.994071, 2015.

Alves, C. A., Vicente, A. M., Custódio, D., Cerqueira, M., Nunes, T., Pio, C., Lucarelli, F., Calzolai, G., Nava, S., Diapouli, E., Eleftheriadis, K., Querol, X. and Musa Bandowe, B. A.: Polycyclic aromatic hydrocarbons and their derivatives (nitro-PAHs, oxygenated PAHs, and azaarenes) in PM 2.5 from Southern European cities, Sci. Total Environ., 595, 494–504, doi:10.1016/j.scitotenv.2017.03.256, 2017.

Amato, F., Favez, O., Pandolfi, M., Alastuey, A., Querol, X., Moukhtar, S., Bruge, B., Verlhac, S., Orza, J. A. G., Bonnaire, N., Le Priol, T., Petit, J.-F. and Sciare, J.: Traffic induced particle resuspension in Paris: Emission factors and source contributions, Atmos. Environ., 129, 114–124, doi:10.1016/j.atmosenv.2016.01.022, 2016.

Anastasopoulos, A. T., Wheeler, A. J., Karman, D. and Kulka, R. H.: Intraurban concentrations, spatial variability and correlation of ambient polycyclic aromatic hydrocarbons (PAH) and PM2.5, Atmos. Environ., 59, 272–283, doi:10.1016/j.atmosenv.2012.05.004, 2012.

Andreou, G. and Rapsomanikis, S.: Polycyclic aromatic hydrocarbons and their oxygenated derivatives in the urban atmosphere of Athens, J. Hazard. Mater., 172(1), 363–373, doi:10.1016/j.jhazmat.2009.07.023, 2009.

Bandowe, B. A. M., Meusel, H., Huang, R., Ho, K., Cao, J., Hoffmann, T. and Wilcke, W.: PM2.5-bound oxygenated PAHs, nitro-PAHs and parent-PAHs from the atmosphere of a Chinese megacity: Seasonal variation, sources and cancer risk assessment, Sci. Total Environ., 473–474, 77–87, doi:10.1016/j.scitotenv.2013.11.108, 2014.

Bernardoni, V., Calzolai, G., Chiari, M., Fedi, M., Lucarelli, F., Nava, S., Piazzalunga, A., Riccobono, F., Taccetti, F., Valli, G. and Vecchi, R.: Radiocarbon analysis on organic and elemental carbon in aerosol samples and source apportionment at an urban site in Northern Italy, J. Aerosol Sci., 56, 88–99, doi:10.1016/j.jaerosci.2012.06.001, 2013.

Boschetti, L., Sparks, A., Roy, D.P., Giglio, L., San-Miguel-Ayanz, J., GWIS national and sub-national fire activity data from the NASA MODIS Collection 6 Burned Area Product in support of policy making, carbon inventories and natural resource management, developed under NASA Applied Sciences grant #80NSSC18K0400, Using the NASA Polar Orbiting Fire Product Record to Enhance and Expand the Global Wildfire Information System (GWIS). **https://gwis.jrc.ec.europa.eu/apps/country.profile/downloads (last accessed on 19 August 2021)**

Brown, S. G., Eberly, S., Paatero, P. and Norris, G. A.: Methods for estimating uncertainty in PMF solutions: Examples with ambient air and water quality data and guidance on reporting PMF results, Sci. Total Environ., 518–519, 626–635, doi:10.1016/j.scitotenv.2015.01.022, 2015.

Buzcu-Guven, B., Brown, S. G., Frankel, A., Hafner, H. R. and Roberts, P. T.: Analysis and Apportionment of Organic Carbon and Fine Particulate Matter Sources at Multiple Sites in the Midwestern United States, J. Air Waste Manage. Assoc., 57(5), 606–619, doi:10.3155/1047-3289.57.5.606, 2007.

Callén, M. S., de la Cruz, M. T., López, J. M., Navarro, M. V. and Mastral, A. M.: Comparison of receptor models for source apportionment of the PM10 in Zaragoza (Spain), Chemosphere, 76(8), 1120–1129, doi:10.1016/j.chemosphere.2009.04.015, 2009.

Cerqueira, M. and Matos, J.: A one-year record of particle-bound polycyclic aromatic hydrocarbons at an urban background site in Lisbon Metropolitan Area, Portugal, Sci. Total Environ., 658, 34–41, doi:10.1016/j.scitotenv.2018.12.151, 2019.

Chen, P., Kang, S., Li, C., Li, Q., Yan, F., Guo, J., Ji, Z., Zhang, Q., Hu, Z., Tripathee, L. and Sillanpää, M.: Source Apportionment and Risk Assessment of Atmospheric Polycyclic Aromatic Hydrocarbons in Lhasa, Tibet, China, Aerosol Air Qual. Res., 18(5), 1294–1304, doi:10.4209/aaqr.2017.12.0603, 2018.

Diapouli, E., Manousakas, M., Vratolis, S., Vasilatou, V., Maggos, T., Saraga, D., Grigoratos, T., Argyropoulos, G., Voutsa, D., Samara, C. and Eleftheriadis, K.: Evolution of air pollution source contributions over one decade, derived by PM10 and PM2.5 source apportionment in two metropolitan urban areas in Greece, Atmos. Environ., 164, 416–430, doi:10.1016/j.atmosenv.2017.06.016, 2017.

Dvorská, A., Lammel, G. and Klánová, J.: Use of diagnostic ratios for studying source apportionment and reactivity of ambient polycyclic aromatic hydrocarbons over Central Europe, Atmos. Environ., 45(2), 420–427, doi:10.1016/j.atmosenv.2010.09.063, 2011.

Fourtziou, L., Liakakou, E., Stavroulas, I., Theodosi, C., Zarmpas, P., Psiloglou, B., Sciare, J., Maggos, T., Bairachtari, K., Bougiatioti, A., Gerasopoulos, E., Sarda-Estève, R., Bonnaire, N. and Mihalopoulos, N.: Multi-tracer approach to characterize domestic wood burning in Athens (Greece) during wintertime, Atmos. Environ., 148(November), 89–101, doi:10.1016/j.atmosenv.2016.10.011, 2017.

Grivas, G., Cheristanidis, S. and Chaloulakou, A.: Elemental and organic carbon in the urban environment of Athens. Seasonal and diurnal variations and estimates of secondary organic carbon, Sci. Total Environ., 414, 535–545, doi:10.1016/j.scitotenv.2011.10.058, 2012.

Grivas, G., Cheristanidis, S., Chaloulakou, A., Koutrakis, P. and Mihalopoulos, N.: Elemental Composition and Source Apportionment of Fine and Coarse Particles at Traffic and Urban Background Locations in Athens, Greece, Aerosol Air Qual. Res., 18(7), 1642–1659, doi:10.4209/aaqr.2017.12.0567, 2018.

Grivas, G., Stavroulas, I., Liakakou, E., Kaskaoutis, D. G., Bougiatioti, A., Paraskevopoulou, D., Gerasopoulos, E. and Mihalopoulos, N.: Measuring the spatial variability of black carbon in Athens during wintertime, Air Qual. Atmos. Heal., 12(12), 1405–1417, doi:10.1007/s11869-019-00756-y, 2019.

Han, D., Fu, Q., Gao, S., Li, L., Ma, Y., Qiao, L., Xu, H., Liang, S., Cheng, P., Chen, X., Zhou, Y., Yu, J. Z. and Cheng, J.: Non-polar organic compounds in autumn and winter aerosols in a typical city of eastern China: size distribution and impact of gas–particle partitioning on PM_{2.5} source apportionment, Atmos. Chem. Phys., 18(13), 9375–9391, doi:10.5194/acp-18-9375-2018, 2018.

Hasheminassab, S., Daher, N., Saffari, A., Wang, D., Ostro, B. D. and Sioutas, C.: Spatial and temporal variability of sources of ambient fine particulate matter (PM2.5) in California, Atmos. Chem. Phys., 14(22), 12085–12097, doi:10.5194/acp-14-12085-2014, 2014.

Iakovides, M., Stephanou, E. G., Apostolaki, M., Hadjicharalambous, M., Evans, J. S., Koutrakis, P. and Achilleos, S.: Study of the occurrence of airborne Polycyclic Aromatic Hydrocarbons associated with respirable particles in two coastal cities at Eastern Mediterranean: Levels, source apportionment, and potential risk for human health, Atmos. Environ., 213(May), 170–184, doi:10.1016/j.atmosenv.2019.05.059, 2019.

Jedynska, A., Hoek, G., Eeftens, M., Cyrys, J., Keuken, M., Ampe, C., Beelen, R., Cesaroni, G., Forastiere, F., Cirach, M., de Hoogh, K., De Nazelle, A., Madsen, C., Declercq, C., Eriksen, K. T., Katsouyanni, K., Akhlaghi, H. M., Lanki, T., Meliefste, K., Nieuwenhuijsen, M., Oldenwening, M., Pennanen, A., Raaschou-Nielsen, O., Brunekreef, B. and Kooter, I. M.: Spatial variations of PAH, hopanes/steranes and EC/OC concentrations within and between European study areas, Atmos. Environ., 87, 239–248, doi:10.1016/j.atmosenv.2014.01.026, 2014.

Jung, K. H., Yan, B., Chillrud, S. N., Perera, F. P., Whyatt, R., Camann, D., Kinney, P. L. and Miller, R. L.: Assessment of Benzo(a)pyrene-equivalent Carcinogenicity and Mutagenicity of Residential Indoor versus Outdoor Polycyclic Aromatic Hydrocarbons Exposing Young Children in New York City, Int. J. Environ. Res. Public Health, 7(5), 1889–1900, doi:10.3390/ijerph7051889, 2010.

Kanellopoulos, P. G., Chrysochou, E., Koukoulakis, K. and Bakeas, E.: Secondary organic aerosol markers and related polar organic compounds in summer aerosols from a sub-urban site in Athens: Size

distributions, diurnal trends and source apportionment, Atmos. Pollut. Res., 12(4), 1–13, doi:10.1016/j.apr.2021.02.013, 2021.

Karagulian, F., Belis, C. A., Dora, C. F. C., Prüss-Ustün, A. M., Bonjour, S., Adair-Rohani, H. and Amann, M.: Contributions to cities' ambient particulate matter (PM): A systematic review of local source contributions at global level, Atmos. Environ., 120, 475–483, doi:10.1016/j.atmosenv.2015.08.087, 2015.

Kaskaoutis, D. G., Grivas, G., Theodosi, C., Tsagkaraki, M., Paraskevopoulou, D., Stavroulas, I., Liakakou, E., Gkikas, A., Hatzianastassiou, N., Wu, C., Gerasopoulos, E. and Mihalopoulos, N.: Carbonaceous Aerosols in Contrasting Atmospheric Environments in Greek Cities: Evaluation of the EC-tracer Methods for Secondary Organic Carbon Estimation, Atmosphere (Basel)., 11(2), 161, doi:10.3390/atmos11020161, 2020.

Kaskaoutis, D. G., Grivas, G., Stavroulas, I., Liakakou, E., Dumka, U. C., Dimitriou, K., Gerasopoulos, E. and Mihalopoulos, N.: In situ identification of aerosol types in Athens, Greece, based on long-term optical and on online chemical characterization, Atmos. Environ., 246, 118070, doi:10.1016/j.atmosenv.2020.118070, 2021.

Katsoyiannis, A., Sweetman, A. J. and Jones, K. C.: PAH Molecular Diagnostic Ratios Applied to Atmospheric Sources: A Critical Evaluation Using Two Decades of Source Inventory and Air Concentration Data from the UK, Environ. Sci. Technol., 45(20), 8897–8906, doi:10.1021/es202277u, 2011.

Khan, M. F., Latif, M. T., Lim, C. H., Amil, N., Jaafar, S. A., Dominick, D., Mohd Nadzir, M. S., Sahani, M. and Tahir, N. M.: Seasonal effect and source apportionment of polycyclic aromatic hydrocarbons in PM2.5, Atmos. Environ., 106, 178–190, doi:10.1016/j.atmosenv.2015.01.077, 2015.

Koukoulakis, K. G., Kanellopoulos, P. G., Chrysochou, E., Costopoulou, D., Vassiliadou, I., Leondiadis, L. and Bakeas, E.: Atmospheric Concentrations and Health Implications of PAHs, PCBs and PCDD/Fs in the Vicinity of a Heavily Industrialized Site in Greece, Appl. Sci., 10(24), 9023, doi:10.3390/app10249023, 2020.

Kozielska, B., Rogula-Kozłowska, W. and Klejnowski, K.: Seasonal Variations in Health Hazards from Polycyclic Aromatic Hydrocarbons Bound to Submicrometer Particles at Three Characteristic Sites in the Heavily Polluted Polish Region, Atmosphere (Basel)., 6(1), 1–20, doi:10.3390/atmos6010001, 2014.

Křůmal, K., Mikuška, P. and Večeřa, Z.: Polycyclic aromatic hydrocarbons and hopanes in PM1 aerosols in urban areas, Atmos. Environ., 67, 27–37, doi:10.1016/j.atmosenv.2012.10.033, 2013.

Lee, S., Liu, W., Wang, Y., Russell, A. G. and Edgerton, E. S.: Source apportionment of PM2.5: Comparing PMF and CMB results for four ambient monitoring sites in the southeastern United States, Atmos. Environ., 42(18), 4126–4137, doi:10.1016/j.atmosenv.2008.01.025, 2008.

Lhotka, R., Pokorná, P. and Zíková, N.: Long-Term Trends in PAH Concentrations and Sources at Rural Background Site in Central Europe, Atmosphere (Basel)., 10(11), 687, doi:10.3390/atmos10110687, 2019.

Li, F., Schnelle-Kreis, J., Cyrys, J., Karg, E., Gu, J., Abbaszade, G., Orasche, J., Peters, A. and Zimmermann, R.: Organic speciation of ambient quasi-ultrafine particulate matter (PM0.36) in Augsburg, Germany: Seasonal variability and source apportionment, Sci. Total Environ., 615, 828–837, doi:10.1016/j.scitotenv.2017.09.158, 2018.

Liakakou, E., Stavroulas, I., Kaskaoutis, D. G., Grivas, G., Paraskevopoulou, D., Dumka, U. C., Tsagkaraki, M., Bougiatioti, A., Oikonomou, K., Sciare, J., Gerasopoulos, E. and Mihalopoulos, N.: Long-term variability, source apportionment and spectral properties of black carbon at an urban background site in Athens, Greece, Atmos. Environ., 222, 117137, doi:10.1016/j.atmosenv.2019.117137, 2020.

Lin, Y., Ma, Y., Qiu, X., Li, R., Fang, Y., Wang, J., Zhu, Y. and Hu, D.: Sources, transformation, and health implications of PAHs and their nitrated, hydroxylated, and oxygenated derivatives in PM 2.5 in Beijing, J. Geophys. Res. Atmos., 120(14), 7219–7228, doi:10.1002/2015JD023628, 2015.

Liu, B., Xue, Z., Zhu, X. and Jia, C.: Long-term trends (1990–2014), health risks, and sources of atmospheric polycyclic aromatic hydrocarbons (PAHs) in the U.S., Environ. Pollut., 220, 1171–1179, doi:10.1016/j.envpol.2016.11.018, 2017.

Mandalakis, M., Tsapakis, M., Tsoga, A. and Stephanou, E. G.: Gas–particle concentrations and distribution of aliphatic hydrocarbons, PAHs, PCBs and PCDD/Fs in the atmosphere of Athens (Greece), Atmos. Environ., 36(25), 4023–4035, doi:10.1016/S1352-2310(02)00362-X, 2002.

Manoli, E., Voutsa, D. and Samara, C.: Chemical characterization and source identification/apportionment of fine and coarse air particles in Thessaloniki, Greece, Atmos. Environ., 36(6), 949–961, doi:10.1016/S1352-2310(01)00486-1, 2002.

Manoli, E., Kouras, A., Karagkiozidou, O., Argyropoulos, G., Voutsa, D. and Samara, C.: Polycyclic aromatic hydrocarbons (PAHs) at traffic and urban background sites of northern Greece: source apportionment of ambient PAH levels and PAH-induced lung cancer risk, Environ. Sci. Pollut. Res., 23(4), 3556–3568, doi:10.1007/s11356-015-5573-5, 2016.

Mantis, J., Chaloulakou, A. and Samara, C.: PM10-bound polycyclic aromatic hydrocarbons (PAHs) in the Greater Area of Athens, Greece, Chemosphere, 59(5), 593–604, doi:10.1016/j.chemosphere.2004.10.019, 2005.

Mao, S., Li, J., Cheng, Z., Zhong, G., Li, K., Liu, X. and Zhang, G.: Contribution of Biomass Burning to Ambient Particulate Polycyclic Aromatic Hydrocarbons at a Regional Background Site in East China, Environ. Sci. Technol. Lett., 5(2), 56–61, doi:10.1021/acs.estlett.8b00001, 2018.

Marino, F., Cecinato, A. and Siskos, P. A.: Nitro-PAH in ambient particulate matter in the atmosphere of Athens, Chemosphere, 40(5), 533–537, doi:10.1016/S0045-6535(99)00308-2, 2000.

Masiol, M., Hofer, A., Squizzato, S., Piazza, R., Rampazzo, G. and Pavoni, B.: Carcinogenic and mutagenic risk associated to airborne particle-phase polycyclic aromatic hydrocarbons: A source apportionment, Atmos. Environ., 60, 375–382, doi:10.1016/j.atmosenv.2012.06.073, 2012.

Masiol, M., Squizzato, S., Formenton, G., Khan, M. B., Hopke, P. K., Nenes, A., Pandis, S. N., Tositti, L., Benetello, F., Visin, F. and Pavoni, B.: Hybrid multiple-site mass closure and source apportionment of PM2.5 and aerosol acidity at major cities in the Po Valley, Sci. Total Environ., 704, 135287, doi:10.1016/j.scitotenv.2019.135287, 2020.

Mirante, F., Alves, C., Pio, C., Pindado, O., Perez, R., Revuelta, M. A. and Artiñano, B.: Organic composition of size segregated atmospheric particulate matter, during summer and winter sampling campaigns at representative sites in Madrid, Spain, Atmos. Res., 132–133, 345–361, doi:10.1016/j.atmosres.2013.07.005, 2013.

Miura, K., Shimada, K., Sugiyama, T., Sato, K., Takami, A., Chan, C. K., Kim, I. S., Kim, Y. P., Lin, N.-H. and Hatakeyama, S.: Seasonal and annual changes in PAH concentrations in a remote site in the Pacific Ocean, Sci. Rep., 9(1), 12591, doi:10.1038/s41598-019-47409-9, 2019.

Myriokefalitakis, S., Tsigaridis, K., Mihalopoulos, N., Sciare, J., Nenes, A., Kawamura, K., Segers, A. and Kanakidou, M.: In-cloud oxalate formation in the global troposphere: a 3-D modeling study, Atmos. Chem. Phys., 11(12), 5761–5782, doi:10.5194/acp-11-5761-2011, 2011.

Norris, G., R. Duvall, S. Brown, and S. Bai. EPA Positive Matrix Factorization (PMF) 5.0 Fundamentals and User Guide. U.S. Environmental Protection Agency, Washington, DC, EPA/600/R-14/108 (NTIS PB2015-105147) (2014)., n.d.

Paatero, P.: The Multilinear Engine—A Table-Driven, Least Squares Program for Solving Multilinear Problems, Including the n -Way Parallel Factor Analysis Model, J. Comput. Graph. Stat., 8(4), 854–888, doi:10.1080/10618600.1999.10474853, 1999.

Paatero, P. and Hopke, P. K.: Discarding or downweighting high-noise variables in factor analytic models, Anal. Chim. Acta, 490(1–2), 277–289, doi:10.1016/S0003-2670(02)01643-4, 2003.

Paatero, P. and Tapper, U.: Positive matrix factorization: A non-negative factor model with optimal utilization of error estimates of data values, Environmetrics, 5(2), 111–126, doi:10.1002/env.3170050203, 1994.

Paatero, P., Eberly, S., Brown, S. G. and Norris, G. A.: Methods for estimating uncertainty in factor analytic solutions, Atmos. Meas. Tech., 7(3), 781–797, doi:10.5194/amt-7-781-2014, 2014.

Pankow, J. F.: An absorption model of the gas/aerosol partitioning involved in the formation of secondary organic aerosol, Atmos. Environ., 28(2), 189–193, doi:10.1016/1352-2310(94)90094-9, 1994.

Paraskevopoulou, D., Liakakou, E., Gerasopoulos, E. and Mihalopoulos, N.: Sources of atmospheric aerosol from long-term measurements (5years) of chemical composition in Athens, Greece, Sci. Total Environ., 527–528, 165–178, doi:10.1016/j.scitotenv.2015.04.022, 2015.

Parinos, C., Hatzianestis, I., Chourdaki, S., Plakidi, E. and Gogou, A.: Imprint and short-term fate of the Agia Zoni II tanker oil spill on the marine ecosystem of Saronikos Gulf, Sci. Total Environ., 693, 133568, doi:10.1016/j.scitotenv.2019.07.374, 2019.

Park, S.-U., Kim, J.-G., Jeong, M.-J. and Song, B.-J.: Source Identification of Atmospheric Polycyclic Aromatic Hydrocarbons in Industrial Complex Using Diagnostic Ratios and Multivariate Factor Analysis, Arch. Environ. Contam. Toxicol., 60(4), 576–589, doi:10.1007/s00244-010-9567-5, 2011.

Pateraki, S., Fameli, K.-M., Assimakopoulos, V., Bougiatioti, A., Maggos, T. and Mihalopoulos, N.: Levels, Sources and Health Risk of PM2.5 and PM1-Bound PAHs across the Greater Athens Area: The Role of the Type of Environment and the Meteorology, Atmosphere (Basel)., 10(10), 622, doi:10.3390/atmos10100622, 2019a.

Pateraki, S., Manousakas, M., Bairachtari, K., Kantarelou, V., Eleftheriadis, K., Vasilakos, C., Assimakopoulos, V. D. and Maggos, T.: The traffic signature on the vertical PM profile: Environmental and health risks within an urban roadside environment, Sci. Total Environ., 646, 448–459, doi:10.1016/j.scitotenv.2018.07.289, 2019b.

Piletic, I. R., Offenberg, J. H., Olson, D. A., Jaoui, M., Krug, J., Lewandowski, M., Turlington, J. M. and Kleindienst, T. E.: Constraining carbonaceous aerosol sources in a receptor model by including 14C data with redox species, organic tracers, and elemental/organic carbon measurements, Atmos. Environ., 80, 216–225, doi:10.1016/j.atmosenv.2013.07.062, 2013.

Polissar, A. V, Hopke, P. K., Paatero, P., Malm, W. C. and Sisler, J. F.: Atmospheric aerosol over Alaska: 2. Elemental composition and sources, J. Geophys. Res. Atmos., 103(D15), 19045–19057, doi:10.1029/98JD01212, 1998.

Ravindra, K., Sokhi, R. and Van Grieken, R.: Atmospheric polycyclic aromatic hydrocarbons: Source attribution, emission factors and regulation, Atmos. Environ., 42(13), 2895–2921, doi:10.1016/j.atmosenv.2007.12.010, 2008.

Romonosky, D. E., Ali, N. N., Saiduddin, M. N., Wu, M., Lee, H. J. (Julie), Aiona, P. K. and Nizkorodov, S. A.: Effective absorption cross sections and photolysis rates of anthropogenic and biogenic secondary organic aerosols, Atmos. Environ., 130, 172–179, doi:10.1016/j.atmosenv.2015.10.019, 2016.

Roux, M. V., Temprado, M., Chickos, J. S. and Nagano, Y.: Critically Evaluated Thermochemical Properties of Polycyclic Aromatic Hydrocarbons, J. Phys. Chem. Ref. Data, 37(4), 1855–1996, doi:10.1063/1.2955570, 2008.

Saarnio, K., Sillanpää, M., Hillamo, R., Sandell, E., Pennanen, A. S. and Salonen, R. O.: Polycyclic aromatic hydrocarbons in size-segregated particulate matter from six urban sites in Europe, Atmos. Environ., 42(40), 9087–9097, doi:10.1016/j.atmosenv.2008.09.022, 2008.

Saffari, A., Daher, N., Samara, C., Voutsa, D., Kouras, A., Manoli, E., Karagkiozidou, O., Vlachokostas, C., Moussiopoulos, N., Shafer, M. M., Schauer, J. J. and Sioutas, C.: Increased Biomass Burning Due to the Economic Crisis in Greece and Its Adverse Impact on Wintertime Air Quality in Thessaloniki, Environ. Sci. Technol., 47(23), 13313–13320, doi:10.1021/es403847h, 2013.

Saraga, D., Maggos, T., Degrendele, C., Klánová, J., Horvat, M., Kocman, D., Kanduč, T., Garcia Dos Santos, S., Franco, R., Gómez, P. M., Manousakas, M., Bairachtari, K., Eleftheriadis, K., Kermenidou, M., Karakitsios, S., Gotti, A. and Sarigiannis, D.: Multi-city comparative PM2.5 source apportionment for fifteen sites in Europe: The ICARUS project, Sci. Total Environ., 751, 141855,

doi:10.1016/j.scitotenv.2020.141855, 2021.

Shen, G., Chen, Y., Wei, S., Fu, X., Ding, A., Wu, H. and Tao, S.: Can Coronene and/or Benzo(a)pyrene/Coronene ratio act as unique markers for vehicle emission?, Environ. Pollut., 184, 650–653, doi:10.1016/j.envpol.2013.08.020, 2014.

Shirmohammadi, F., Hasheminassab, S., Saffari, A., Schauer, J. J., Delfino, R. J. and Sioutas, C.: Fine and ultrafine particulate organic carbon in the Los Angeles basin: Trends in sources and composition, Sci. Total Environ., 541, 1083–1096, doi:10.1016/j.scitotenv.2015.09.133, 2016.

Sitaras, I. E. and Siskos, P. A.: Levels of Volatile Polycyclic Aromatic Hydrocarbons in the Atmosphere of Athens, Greece, Polycycl. Aromat. Compd., 18(4), 451–467, doi:10.1080/10406630108233820, 2001.

Sofowote, U. M., McCarry, B. E. and Marvin, C. H.: Source Apportionment of PAH in Hamilton Harbour Suspended Sediments: Comparison of Two Factor Analysis Methods, Environ. Sci. Technol., 42(16), 6007–6014, doi:10.1021/es800219z, 2008.

Srivastava, D., Favez, O., Perraudin, E., Villenave, E. and Albinet, A.: Comparison of Measurement-Based Methodologies to Apportion Secondary Organic Carbon (SOC) in PM2.5: A Review of Recent Studies, Atmosphere (Basel)., 9(11), 452, doi:10.3390/atmos9110452, 2018a.

Srivastava, D., Favez, O., Bonnaire, N., Lucarelli, F., Haeffelin, M., Perraudin, E., Gros, V., Villenave, E. and Albinet, A.: Speciation of organic fractions does matter for aerosol source apportionment. Part 2: Intensive short-term campaign in the Paris area (France), Sci. Total Environ., 634, 267–278, doi:10.1016/j.scitotenv.2018.03.296, 2018b.

Stavroulas, I., Bougiatioti, A., Grivas, G., Paraskevopoulou, D., Tsagkaraki, M., Zarmpas, P., Liakakou, E., Gerasopoulos, E. and Mihalopoulos, N.: Sources and processes that control the submicron organic aerosol composition in an urban Mediterranean environment (Athens): a high temporal-resolution chemical composition measurement study, Atmos. Chem. Phys., 19(2), 901–919, doi:10.5194/acp-19-901-2019, 2019.

Sulong, N. A., Latif, M. T., Sahani, M., Khan, M. F., Fadzil, M. F., Tahir, N. M., Mohamad, N., Sakai, N., Fujii, Y., Othman, M. and Tohno, S.: Distribution, sources and potential health risks of polycyclic aromatic hydrocarbons (PAHs) in PM2.5 collected during different monsoon seasons and haze episode in Kuala Lumpur, Chemosphere, 219, 1–14, doi:10.1016/j.chemosphere.2018.11.195, 2019.

Taghvaee, S., Sowlat, M. H., Mousavi, A., Hassanvand, M. S., Yunesian, M., Naddafi, K. and Sioutas, C.: Source apportionment of ambient PM2.5 in two locations in central Tehran using the Positive Matrix Factorization (PMF) model, Sci. Total Environ., 628–629, 672–686, doi:10.1016/j.scitotenv.2018.02.096, 2018.

Theodosi, C., Tsagkaraki, M., Zarmpas, P., Grivas, G., Liakakou, E., Paraskevopoulou, D., Lianou, M., Gerasopoulos, E. and Mihalopoulos, N.: Multi-year chemical composition of the fine-aerosol fraction in Athens, Greece, with emphasis on the contribution of residential heating in wintertime, Atmos. Chem. Phys., 18(19), 14371–14391, doi:10.5194/acp-18-14371-2018, 2018.

Valavanidis, A., Fiotakis, K., Vlahogianni, T., Bakeas, E. B., Triantafillaki, S., Paraskevopoulou, V. and Dassenakis, M.: Characterization of atmospheric particulates, particle-bound transition metals and polycyclic aromatic hydrocarbons of urban air in the centre of Athens (Greece), Chemosphere, 65(5), 760–768, doi:10.1016/j.chemosphere.2006.03.052, 2006.

Valotto, G., Rampazzo, G., Gonella, F., Formenton, G., Ficotto, S. and Giraldo, G.: Source apportionment of PAHs and n -alkanes bound to PM 1 collected near the Venice highway, J. Environ. Sci., 54, 77–89, doi:10.1016/j.jes.2016.05.025, 2017.

Vasilakos, C., Levi, N., Maggos, T., Hatzianestis, J., Michopoulos, J. and Helmis, C.: Gas–particle concentration and characterization of sources of PAHs in the atmosphere of a suburban area in Athens, Greece, J. Hazard. Mater., 140(1–2), 45–51, doi:10.1016/j.jhazmat.2006.06.047, 2007.

Viras, L. G. and Siskos, P. A.: Spatial and Time Variation and Effect of Some Meteorological Parameters in Polycyclic Aromatic Hydrocarbons in Athens Greece, Polycycl. Aromat. Compd., 3(2), 89–100, doi:10.1080/10406639308047861, 1993.

Viras, L. G., Siskos, P. A. and Stephanou, E.: Determination of Polycyclic Aromatic Hydrocarbons in Athens Atmosphere, Int. J. Environ. Anal. Chem., 28(1–2), 71–85, doi:10.1080/03067318708078400, 1987.

Viras, L. G., Athanasiou, K. and Siskos, P. A.: Determination of mutagenic activity of airborne particulates and of the benzo[α]pyrene concentrations in Athens atmosphere, Atmos. Environ. Part B. Urban Atmos., 24(2), 267–274, doi:10.1016/0957-1272(90)90032-P, 1990.

Vogel, A. L., Schneider, J., Müller-Tautges, C., Klimach, T. and Hoffmann, T.: Aerosol Chemistry Resolved by Mass Spectrometry: Insights into Particle Growth after Ambient New Particle Formation, Environ. Sci. Technol., 50(20), 10814–10822, doi:10.1021/acs.est.6b01673, 2016.

Wang, F., Lin, T., Li, Y., Ji, T., Ma, C. and Guo, Z.: Sources of polycyclic aromatic hydrocarbons in PM2.5 over the East China Sea, a downwind domain of East Asian continental outflow, Atmos. Environ., 92, 484–492, doi:10.1016/j.atmosenv.2014.05.003, 2014.

Wang, L., Zhao, Y., Yi, X., Wang, Z., Yi, Y., Huang, T., Gao, H. and Ma, J.: Spatial distribution of atmospheric PAHs and their genotoxicity in petrochemical industrialized Lanzhou valley, northwest China, Environ. Sci. Pollut. Res., 24(14), 12820–12834, doi:10.1007/s11356-017-8808-9, 2017.

Wang, Q., Feng, Y., Huang, X. H. H., Griffith, S. M., Zhang, T., Zhang, Q., Wu, D. and Yu, J. Z.: Nonpolar organic compounds as PM 2.5 source tracers: Investigation of their sources and degradation in the Pearl River Delta, China, J. Geophys. Res. Atmos., 121(19), 11,862-11,879, doi:10.1002/2016JD025315, 2016.

Wang, S., Ji, Y., Zhao, J., Lin, Y. and Lin, Z.: Source apportionment and toxicity assessment of PM2.5-bound PAHs in a typical iron-steel industry city in northeast China by PMF-ILCR, Sci. Total Environ., 713, 136428, doi:10.1016/j.scitotenv.2019.136428, 2020.

Williams, B. J., Goldstein, A. H., Kreisberg, N. M. and Hering, S. V: In situ measurements of gas/particle-phase transitions for atmospheric semivolatile organic compounds, Proc. Natl. Acad. Sci., 107(15), 6676–6681, doi:10.1073/pnas.0911858107, 2010.

Xie, M., Barsanti, K. C., Hannigan, M. P., Dutton, S. J. and Vedal, S.: Positive matrix factorization of PM2.5 – eliminating the effects of gas/particle partitioning of semivolatile organic compounds, Atmos. Chem. Phys., 13(15), 7381–7393, doi:10.5194/acp-13-7381-2013, 2013.

Yu, Q., Ding, X., He, Q., Yang, W., Zhu, M., Li, S., Zhang, R., Shen, R., Zhang, Y., Bi, X., Wang, Y., Peng, P. and Wang, X.: Nationwide increase of polycyclic aromatic hydrocarbons in ultrafine particles during winter over China revealed by size-segregated measurements, Atmos. Chem. Phys., 20(23), 14581–14595, doi:10.5194/acp-20-14581-2020, 2020.

Yunker, M. B., Macdonald, R. W., Vingarzan, R., Mitchell, R. H., Goyette, D. and Sylvestre, S.: PAHs in the Fraser River basin: a critical appraisal of PAH ratios as indicators of PAH source and composition, Org. Geochem., 33(4), 489–515, doi:10.1016/S0146-6380(02)00002-5, 2002.

Zhang, Z., Gao, J., Engling, G., Tao, J., Chai, F., Zhang, L., Zhang, R., Sang, X., Chan, C., Lin, Z. and Cao, J.: Characteristics and applications of size-segregated biomass burning tracers in China's Pearl River Delta region, Atmos. Environ., 102, 290–301, doi:10.1016/j.atmosenv.2014.12.009, 2015.

Zheng, X., Wu, Y., Zhang, S., Hu, J., Zhang, K. M., Li, Z., He, L. and Hao, J.: Characterizing particulate polycyclic aromatic hydrocarbon emissions from diesel vehicles using a portable emissions measurement system, Sci. Rep., 7(1), 10058, doi:10.1038/s41598-017-09822-w, 2017.

Zielinska, B., Sagebiel, J., McDonald, J. D., Whitney, K. and Lawson, D. R.: Emission Rates and Comparative Chemical Composition from Selected In-Use Diesel and Gasoline-Fueled Vehicles, J. Air Waste Manage. Assoc., 54(9), 1138–1150, doi:10.1080/10473289.2004.10470973, 2004.